

**Filler Reinforced Elastomers Based on Functional  
Polyolefin Prepolymers**

A THESIS  
SUBMITTED TO THE FACULTY OF  
UNIVERSITY OF MINNESOTA  
BY

Ning Ren

IN PARTIAL FULFILLMENT OF THE REQUIREMENTS  
FOR THE DEGREE OF  
MASTER OF SCIENCE

Marc A. Hillmyer, Advisor

May 2015

© Ning Ren 2015  
ALL RIGHTS RESERVED

## **Acknowledgements**

Firstly, I would like to thank my advisor Professor Marc A. Hillmyer for offering me the chance to work on the polyolefin-filler project and all the guidance on my research during my time at University of Minnesota. I would also like to thank the graduate students, postdocs and undergraduate students who provided help on my research, these people are Dr. Henry Martinez, Dr. Yanzhao Wang, Megan Matta, and all the other members in the Hillmyer group. Finally, the financial support from the Dow Chemical Company and the Department of Chemical Engineering and Materials Science is also acknowledged gratefully.

## **Dedication**

To my parents.

## **Abstract**

Carboxy-telechelic polyethylene prepolymers were synthesized by ring-opening metathesis polymerization of 3-ethyl-1-cyclooctene in the presence of maleic acid followed by hydrogenation. Crosslinking of the prepolymer with a tri-functional crosslinker and fumed silica or carbon black filler yielded polyethylene elastomers with enhanced mechanical properties as compared to the unfilled versions. The tensile strength, modulus and tear strength of the elastomers are tunable by changing the filler content. Further study on the filler reinforcing mechanism suggests that both the polymer-filler interactions and the filler-filler interactions play key roles in the mechanical property enhancement.

## Table of Contents

<b>Acknowledgement</b>	<b>i</b>
<b>Dedication</b>	<b>ii</b>
<b>Abstract</b>	<b>iii</b>
<b>Table of Contents</b>	<b>iv</b>
<b>List of Tables</b>	<b>vi</b>
<b>List of Figures</b>	<b>vii</b>
<b>Chapter 1</b>	
<b>Background: Synthesis and Reinforcement of Polyolefin Elastomers .....</b>	<b>1</b>
1.1 Polyolefin Elastomers .....	2
1.2 Synthesis of Polyolefin Elastomers via ROMP .....	5
1.2.1 Metathesis Reaction and Ring-Opening Metathesis Polymerization .....	5
1.2.2 Catalyst for Ring-Opening Metathesis Polymerization .....	8
1.2.3 Synthesis of Telechelic Polyolefin by ROMP with CTA .....	11
1.2.4 Polyolefin Elastomers based on ROMP .....	14
1.3 Reinforcing Filler .....	16
1.3.1 General Reinforcing Mechanism .....	16
1.3.2 Carbon Black Filler .....	20
1.3.3 Silica Filler .....	21
1.4 Conclusions .....	24
1.5 References .....	25

## Chapter 2

### Synthesis of Polyolefin Elastomers via a ROMP-Hydrogenation-Crosslinking

<b>Method and their Reinforcement with Fillers.....</b>	<b>30</b>
2.1 Introduction .....	31
2.2 Results and Discussion .....	33
2.2.1 Prepolymer Synthesis.....	33
2.2.2 Filler Incorporation and crosslinking of prepolymers .....	35
2.2.3 Morphology Study .....	36
2.2.4 Thermal Properties.....	39
2.2.5 Rheological Properties.....	41
2.2.6 Mechanical Properties.....	47
2.2.7 Reinforcing Mechanism.....	51
2.3 Conclusions.....	54
2.4 Materials and Characterization .....	55
2.4.1 Materials .....	55
2.4.2 Characterization.....	55
2.5 References.....	57
Bibliography .....	59

## **List of Tables**

Table 1.1 Physical properties of saturated poly[(COE)-co-(3-hexyl-1-COE)].....	15
Table 2.1 Filler content and thermal properties of filled elastomers .....	40
Table 2.2 Mechanical properties of filler reinforced prepolymers and LSR .....	48
Table 2.3 Characterization of filler reinforced crosslinked prepolymers .....	52



## List of Figures

Figure 1.1 A dangling chain, loop and entanglement in polymer network.....	3
Figure 1.2 Three main variations of metathesis reaction.....	5
Figure 1.3 Commonly used catalyst for ROMP.....	10
Figure 1.4 Synthesis of ABA triblock polyethylene copolymers via ROMP.....	13
Figure 1.5 Synthesis of carboxy-telechelic poly[(COE)-co-(3-hexyl-1-COE)]. .....	14
Figure 1.6 Relationship between filler's reinforcement effect and particle size .....	18
Figure 1.7 Different contributions to the modulus of elastomers.....	19
Figure 1.8 Surface treatment of the hydrophilic silica particle with TESPT .....	23
Figure 2.1 Filler reinforced elastomers from telechelic polyolefin prepolymers .....	32
Figure 2.2 <sup>1</sup> H NMR characterization of the prepolymer .....	34
Figure 2.3 Representative SEM images of fumed silica and carbon black fillers .....	37
Figure 2.4 Representative SEM images of carbon black filled polyolefin elastomers .....	38
Figure 2.5 Representative SEM images of fumed silica filled polyolefin elastomers .....	38
Figure 2.6 Viscosity of prepolymer-filler mixture .....	41
Figure 2.7 Viscosity of prepolymer-filler mixture and LSR before crosslinking.....	42
Figure 2.8 Dynamic mechanical thermal analysis of silica filled elastomers .....	43
Figure 2.9 Dynamic mechanical thermal analysis of carbon black filled elastomers.....	43
Figure 2.10 Frequency sweep (25 °C) of crosslinked PHEt with fillers .....	44
Figure 2.11 Frequency sweep (25 °C) of crosslinked elastomers and LSR .....	45
Figure 2.12 Oscillation sweep of xPHEt with fumed silica and carbon black filler .....	46
Figure 2.12 Volume fraction-storage modulus relationship of xPHEt with silica filler....	53

# Chapter 1

## Background: Synthesis and Reinforcement of Polyolefin Elastomers

This chapter provides the background for ring-opening metathesis polymerization and its application in the synthesis of telechelic polyolefins which can be crosslinked to prepare polyolefin elastomers. The modification of the synthetic polyolefin elastomers via the reinforcing filler is also discussed in this section.

## 1.1 Polyolefin Elastomers

Elastomers refer to crosslinked polymeric materials with  $T_g$  much lower than room temperature.<sup>1</sup> In general, elastomers have good extensibility, strength, energy absorption and resilience.<sup>2</sup> Elastomer materials like natural rubber, silicone rubber, and polyurethane are widely used in different areas, from commonly used car tires, sealants and soft covers, to advanced medical and electrical device.

Before crosslinking an elastomer can hardly maintain its shape after large deformation.<sup>3</sup> Crosslinking of elastomers into a polymer network can provide enhanced mechanical properties. Commonly used crosslinking methods are based on bridge linking between different polymer chains through: 1) sulfur vulcanization, 2) peroxide curing, and 3)  $\gamma$ -irradiation.<sup>4</sup> However, these methods will lead to a broad mass distribution between crosslinks and the formation of highly complex network structures including dangling chains and loops that will affect the mechanical property of the elastomer. According to statistical mechanical theory, the shear modulus of an ideal elastomer,  $G$ , can be calculated from the following equation:

$$G = kT \frac{\nu_e}{V}$$

in which  $\nu_e$  is the total number of the elastically effective strands,  $k$ ,  $T$ , and  $V$  are Boltzmann constant, temperature, and volume, correspondingly. Dangling chains and loops are defects in the polymer network that will reduce the amount of effective strands so that the shear modulus of the elastomer is lower than that of an ideal case. Figure 1.1 shows the complex network structure formed after crosslinking.

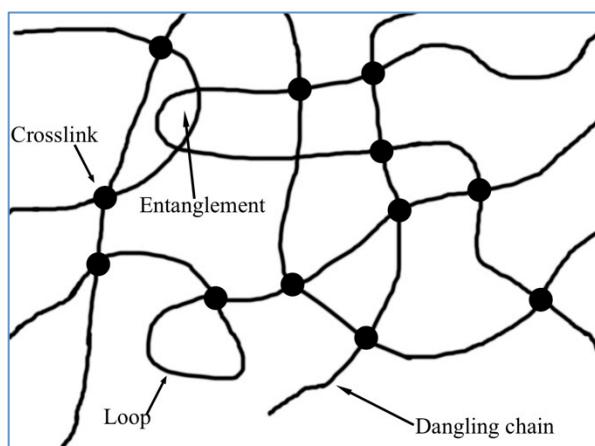


**Figure 1.1**

A dangling chain, loop and entanglement in polymer network.

An alternative method is to crosslink a well-defined linear polymer with functionalized chain ends (telechelic polymer).<sup>4</sup> Multi-functional group agents can be used to crosslink the prepolymer to form a network. Molecular weight between crosslinks is better controlled, because it mainly depends on the molecular weight of the telechelic pre-polymer. The resulting elastomers will also contain a less complex network structure like dangling chains supposing a high conversion for the crosslinking reaction. For example,  $\alpha,\omega$ -divinyl polydimethylsiloxane can be obtained by anionic polymerization of cyclic siloxane.<sup>5</sup> Since it is a telechelic polymer with vinyl-terminated end group, it can be used to crosslink with silicone polymers that have multiple Si-H bonds to prepare silicone rubber through hydrosilylation.<sup>6</sup> This kind of telechelic silicone polymer can be considered a liquid polymer at room temperature since its  $T_g$  is much lower than room temperature, so it is usually called a liquid silicone rubber (LSR). LSR has excellent hydrophobicity, a wide operating temperature range, and high elongation at break. It also has a wide range of applications, including sealing and joint applications.<sup>7</sup>

Besides the commonly used elastomers such as natural rubber and silicone, polyolefin-based elastomers have received considerable interest due to their low cost, easily processible, stable towards chemicals and colorable features.<sup>8</sup> However, polyolefin-based elastomers including polyisobutylene, ethylene propylene rubber (EPR), ethylene propylene diene monomer rubber (EPDM) and polyethylene-octylene rubber are mainly cured by peroxide and irradiation. The synthesis of telechelic polyolefins for elastomers remains challenging. Although advanced polymerization techniques like living radical polymerization and living anionic polymerization allow for synthesis of telechelic polymers (including polystyrene, polymethylmethacrylate, and polydimethylsiloxane), the synthesis of telechelic polyolefins using these methods is mainly restricted to polybutadiene, and the incorporation of functional side group into the telechelic polybutadiene is difficult.<sup>9</sup> So the design of telechelic polyolefins for a crosslinked elastomer that has similar properties as LSR can further broaden the application of polyolefin materials, and will serve as the basis of this thesis.

## 1.2 Synthesis of Polyolefin Prepolymers via ROMP

### 1.2.1 Metathesis Reaction and Ring-Opening Metathesis Polymerization

Olefin metathesis reactions including ring-closing metathesis (RCM), cross-metathesis (CM), acyclic diene metathesis chain-transfer (ADMET) polymerization, and ring-opening metathesis polymerization (ROMP) have gained significant importance with the development of highly active catalysts.<sup>10</sup> In general, olefin metathesis can be divided into three main types: ring opening metathesis, ring closing metathesis and cross metathesis, as summarized in Figure 1.2. Ring opening metathesis refers to the opening of the double bond for a cyclic olefin with considerable ring-strain; ring closing metathesis reaction happens via an intramolecular metathesis reaction to form a cyclic olefin; cross metathesis generally involves the reaction between two acyclic olefins.

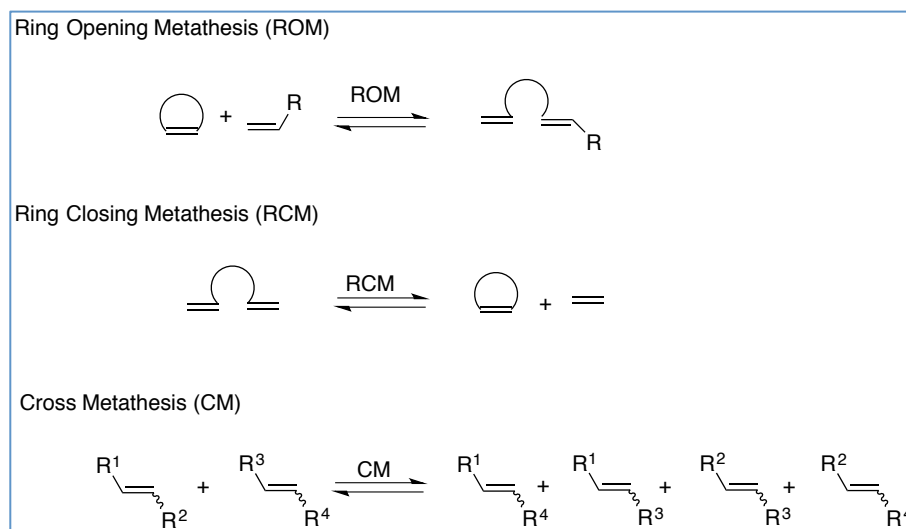
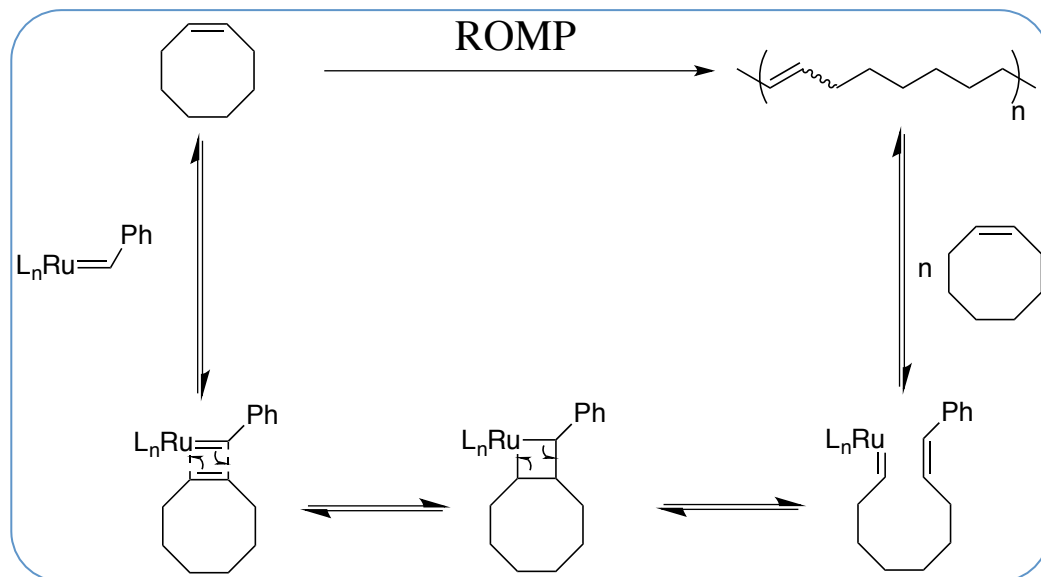


**Figure 1.2**

Three main variations of metathesis reaction: Ring opening metathesis, ring closing metathesis and cross metathesis.

Of the three main types of olefin metathesis reaction, ring-opening metathesis reaction is widely used for the synthesis of polyolefin materials by ring-opening metathesis polymerization, which plays an important role in the field of synthetic polymer chemistry.

Scheme 1.1 shows the well-studied mechanism for the ring-opening metathesis polymerization using cis-cyclooctene (COE) as an example.<sup>11</sup> The first step of the reaction is the formation of a metallocyclobutane intermediate. The intermediate is obtained by the formation of a Dewar-Chat-Duncanson adduct followed by a [2+2] cycloaddition. The metallocyclobutane intermediate will further break down and lead to the formation of the ring-opening olefin product with a metal alkylidene via a retro [2+2] mechanism. The driving force for the reaction is the release of the ring strain of the cyclic olefin, and different conditions including the temperature, concentration and solvent can have significant influence on reaction.<sup>12</sup> However, if the cis-cyclooctene used in this example is replaced by a substituted cyclooctene/cyclooctadiene which is structurally asymmetric, the polymers obtained will possibly contain head-to-head, tail-to-tail and head-to-tail repeat units, and the related regio-selectivity will depend on the type of monomers and catalysts.



**Scheme 1.1**

Mechanism of ring-opening metathesis polymerization with *cis*-cyclooctene and ruthenium catalyst as an example.



## 1.2.2 Catalyst for Ring-Opening Metathesis Polymerization

Katz and coworkers obtained the first well-defined catalyst for the ROMP of cyclooctene in 1976, when researchers began to realize that metal-carbene plays a key role in olefin metathesis.<sup>13</sup> Later on, several other metal alkylidene complexes with high oxidation state were developed as catalysts for olefin metathesis.<sup>14,15</sup> Of them well-defined  $M(=CHtBu)(OtBu)_2(NAr)$ ,  $M(=CHtBu)(OC(CH_3)_2(CF_3))_2(NAr)$ , and  $M(=CHtBu)-(OC(CH_3)(CF_3)_2)_2(NAr)$  ( $NAr = N-2,6-i-Pr_2C_6H_3$ ,  $M = Mo$  or  $W$ ) and their derivatives were important Lewis acid-free ROMP catalysts that show enhanced control over molecular weight and tolerance towards functional group.<sup>12,15,16</sup> Although structurally similar to each other, well-defined Mo-based catalysts are generally applicable to broader range of functional groups compared with W-based catalyst.<sup>12,15</sup> All these catalysts were reported to be active towards ROMP of cyclooctenes.<sup>13,16-19</sup>

In 1992 Noels et.al first reported the ROMP of cis-cyclooctene via ruthenium catalyst that leads to well-understood polyalkenamer structure. A series of ruthenium catalyst including [(p-cymene)RuCl<sub>2</sub>]<sub>2</sub>, Ruthenium(II) trifluoroacetate, and ruthenium(II) with phosphine-substituted complexes were demonstrated to be efficient catalysts with diazoester as initiator.<sup>20</sup> Then, in 1993, Nguyen, Grubbs, and Ziller reported the discovery of (Cy<sub>3</sub>P)<sub>2</sub>Cl<sub>2</sub>Ru=CHCH=CPh<sub>2</sub>, which is structurally very close to Grubbs Generation I catalyst, and the catalyst is the first well defined ruthenium that shows activity for the ROMP of cis-cyclooctene and 1,5-cyclooctadiene.<sup>21</sup> In 1996 Schwab, Grubbs, and Ziller published the synthesis of Grubbs Generation I catalyst and the ROMP

of cis-cyclooctene and 1,5-cyclooctadiene with G1 under room temperature in bulk.<sup>22</sup> The activity of Grubbs Generation II catalyst (G2) towards ROMP of cis-cyclooctene and 1,5-cyclooctadiene was reported by Bielawski and Grubbs in 2000.<sup>23</sup> The NHC ligand in Grubbs G2 is a strong  $\sigma$ -donor and can enhance the stability of the fourteen-electrons intermediate to improve the activity of the catalyst. Hoveyda and coworkers reported the synthesis of recyclable ruthenium catalyst based on Grubbs Generation I, and the catalyst was later called Grubbs-Hoveyda Generation I (GH1).<sup>24</sup> The kinetics studies of GH1 polymerization showed that the initiation rate constant was 30 times slower than Grubbs's G1 and the propagation rate was 4 times faster. The slow initiation step was explained by the less facile dissociation of the isopropyl aryl ether ligand compared to PCy<sub>3</sub>, while the improvement in propagation rate was mainly due to the intermediacy of monophosphine. Based on these classic ruthenium catalysts, other kinds of ruthenium catalyst has been extensively developed during the past decades including Grubbs Generation III (G3)<sup>25</sup>, Grubbs-Hoveyda II (GH2)<sup>26</sup>, and many of them show catalytic activity towards ROMP of cis-cyclooctene<sup>27-30</sup> and 1,5-cyclooctadiene<sup>25,30-34</sup>. Figure 1.3 summarized some of the commonly used catalyst for the ROMP of cyclooctene and cyclooctadiene.

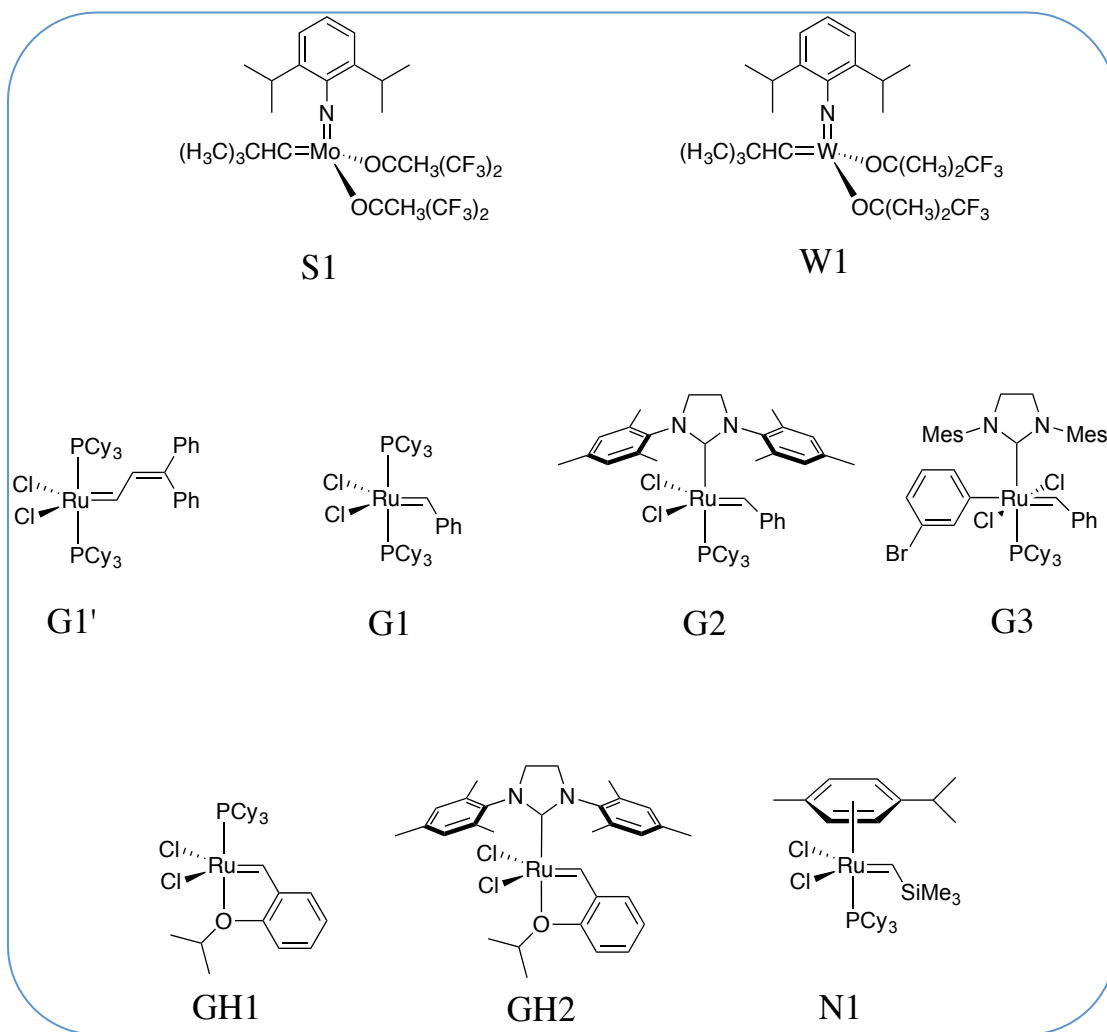
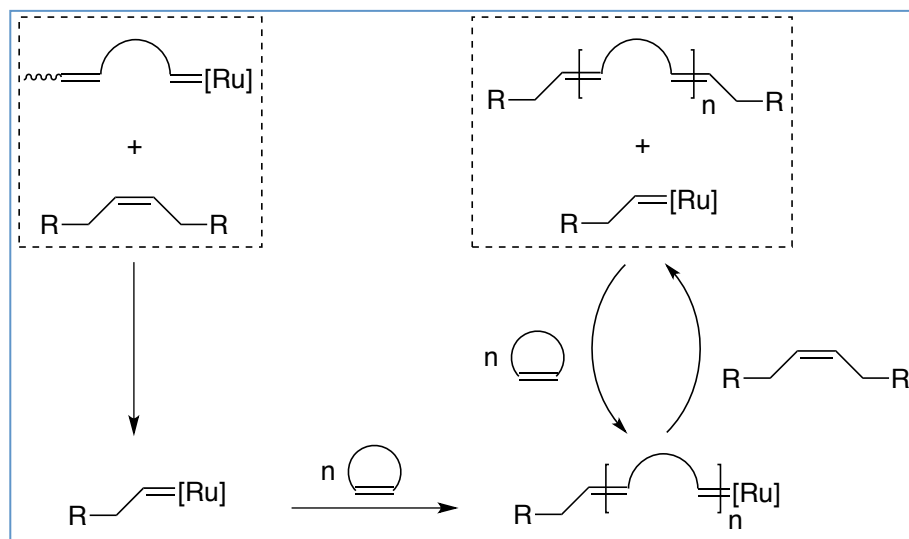


**Figure 1.3**  
Commonly used catalyst for ROMP.

### 1.2.3 Synthesis of Telechelic Polyolefin by ROMP with CTA

ROMP of cyclooctene and cyclooctadiene can be used for the synthesis of polyolefin materials, and the use of di-functional acyclic olefin as a chain transfer agent (CTA) in ROMP has become a powerful and efficient way to prepare telechelic polyolefins.<sup>35</sup> This is achieved by cross-metathesis between the propagating metal-alkylidene intermediate and the CTA, as shown in Scheme 1.2. The molecular weight can be controlled by monomer/CTA mole ratio when the concentration of CTA is much higher than that of the ROMP catalyst.<sup>36</sup>



**Scheme 1.2**  
Mechanism of ring-opening metathesis-chain transfer polymerization.

Various kinds of difunctional acyclic olefins have been reported as the CTA for the ROMP of cyclooctene/cyclooctadiene and their derivatives to synthesize telechelic polyolefin polymers.<sup>37-42</sup> For example, Hillmyer et al. reported that hydroxy-telechelic polybutadiene can be synthesized via ROMP with acetyl protected 1,4-butadiene-diol as

CTA.<sup>42</sup> There was also report on the use of diol without protection as the CTA for the synthesis of polyolefins via ROMP.<sup>43</sup> However, for the synthesis of amino-telechelic polyolefins, due to the fact that amino group can coordinate with the metal center and deactivate the reactivity of catalysts,<sup>44</sup> the use of protecting group is necessary. Morita et al. reported the use of cis-1,4-di-tert-butyl-2-butene-1,4-dicarbamate as the CTA to synthesize amino-telechelic poly(butadiene). Later on Ji et al. used 1,4-dicyano-2-butene as the CTA for the ROMP of 1,5-cyclooctadiene to obtain cyano-telechelic poly(butadiene) and then reduced it to amino-telechelic poly(butadiene).<sup>39</sup> The use of CTA can also help synthesis block copolymers with polyolefin block in the middle.<sup>45,46</sup> Figure 1.4 shows an ABA triblock dendric polyethylene synthesized by ROMP with CTA.<sup>47</sup>

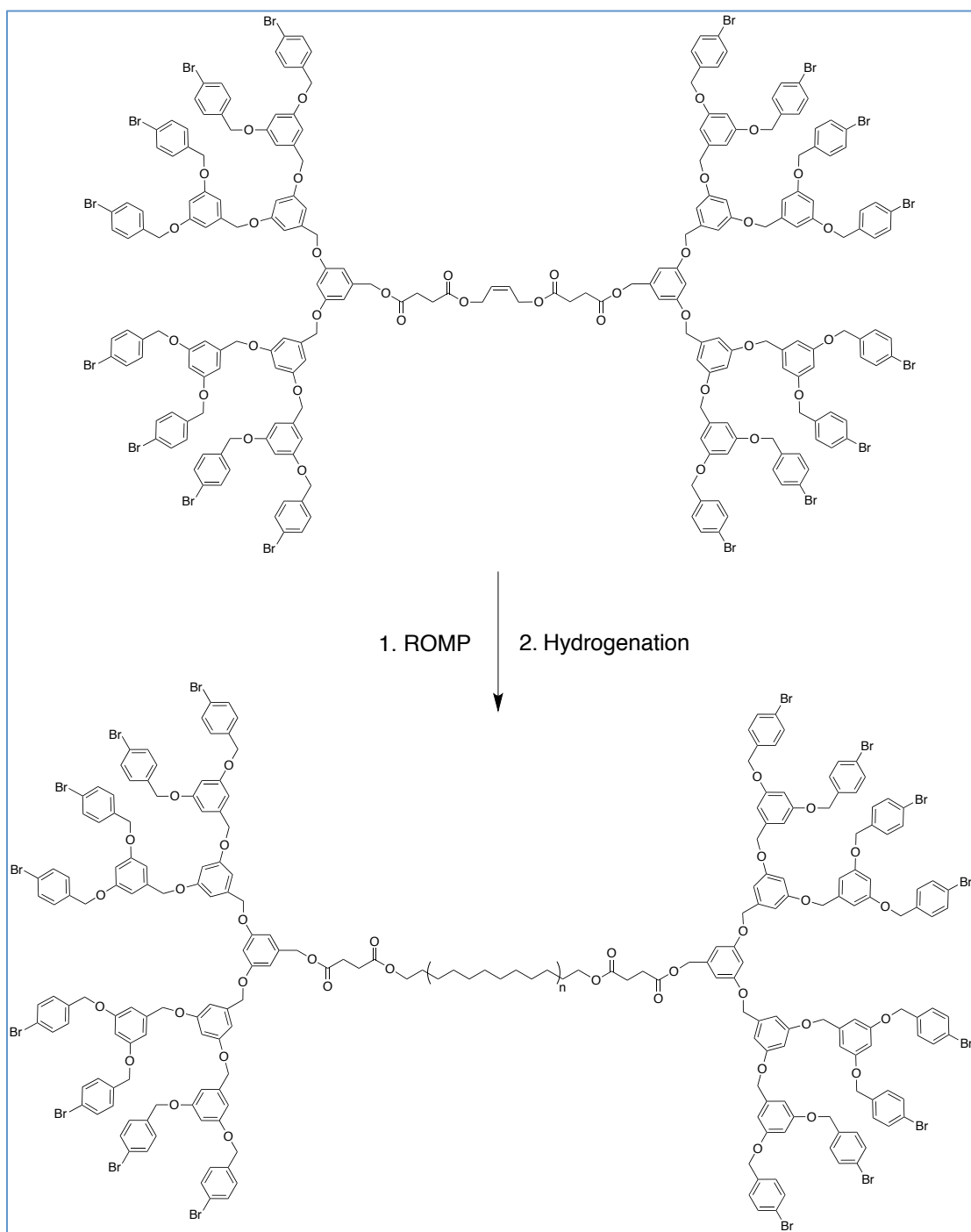


**Figure 1.4**  
Synthesis of ABA triblock polyethylene copolymers via ROMP.<sup>48</sup>

### 1.2.4 Polyolefin Elastomers based on ROMP

Our research group has already demonstrated that carboxy-telechelic polyolefin prepolymers can be prepared via ROMP of cyclooctene and 3-hexyl-1-cyclooctene with maleic acid as the CTA (Figure 1.5).<sup>38,48-50</sup> The use of maleic acid as the CTA without any protection can effectively control the molar mass of the prepolymer and provide end-group functionality around two. The presence of carboxylic group will not influence the reactivity of G2 catalyst and can survive from hydrogenation. The crosslink of carboxy-telechelic prepolymers with tris-aziridine (TAz) is also convenient and efficient.

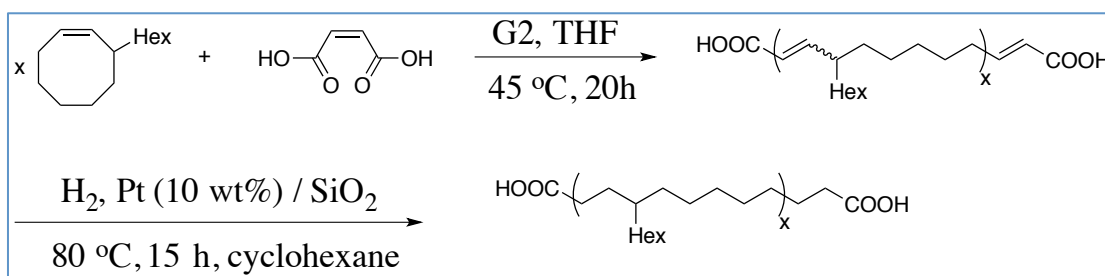


**Figure 1.5**

Synthesis of carboxy-telechelic poly[(COE)-co-(3-hexyl-1-COE)]

Upon hydrogenation to saturate the backbone, telechelic polyethylene with hexyl branches can be obtained. The crystallinity of the saturated polymer can be controlled by ratio between cyclooctene and 3-hexyl-1-cyclooctene. Table 1.1 shows the relationship between the polymer's thermal properties and the number of the hexyl branches along its backbone. Polymers with a higher percentage of hexyl branches have lower crystallinity. For polymers with 50 mol% of 3-hexyl-1-cyclooctene, the crystallinity is reduced to 3%,

which is almost amorphous. With this method, telechelic polyolefins with different functional side chains and end groups can be synthesized by a ROMP-hydrogenation method, and the polymer was then crosslinked by the tri-functional crosslinker TAz to obtain elastomeric materials. However, compared with commercially available LSR, the mechanical properties of the polyethylene elastomers were not at the level of typical LSRs, and in the following section, the effective solutions to enhance the mechanical properties of the synthesized elastomers with fillers will be discussed.

**Table 1.1**  
Physical properties of saturated poly[(COE)-co-(3-hexyl-1-COE)]<sup>50</sup>

Polymer <sup>a</sup>	$M_n$ (kg mol <sup>-1</sup> )	$\bar{D}$	$T_g$ (°C)	$T_m$ (°C)	$T_c$ (°C)	$\Delta H_m$ (J g <sup>-1</sup> )	Crystallinity (%)
PH-0	4.8			132	118	231	83
PH-25	4.5			88	78	51	18
PH-50	5.1	2.10	-58	38	14	7	3
PH-75	4.3	1.92	-66				
PH-100	4.3	1.69	-68				

a) The number after PH- demonstrates the mole percentage of 3-hexyl-1-cyclooctene in the polymer



## 1.3 Reinforcing Filler

Filler, by definition, is a solid material added to polymers to modify their physical and/or chemical properties. Carbon black, fumed silica, TiO<sub>2</sub> particles, clay, carbon fibers, and CaCO<sub>3</sub> are commonly used fillers for polymers to enhance their mechanical, electrical, thermal, magnetic, and optical properties.<sup>51</sup> With the development of nanotechnology, carbon nanotube and graphene are also used as fillers to enhance the properties of elastomers.<sup>52,53</sup>

### 1.3.1 General Reinforcing Mechanism

For the purpose of this thesis, the mechanical properties of elastomers are the main interest, so the discussion in this section will focus on the mechanical properties of reinforced elastomers. In general, the reinforcement of the mechanical properties refers to the change in the elastomer's modulus, tensile strength, tear strength, elongation at break and abrasion resistance.

The basic reinforcing factor of the filler is the hydrodynamic effect, which is due to the addition of rigid filler particles into the polymer matrix. This reinforcing effect can be described with the following equation:

$$G = G_m(1 + 2.5\phi)$$

The equation is known as Einstein-Smallwood formula, in which  $G_m$  is modulus of the elastomer without fillers and  $\phi$  is the volume fraction of the filler.  $G$  is the modulus of the filled elastomer. The equation was first obtained by Einstein to describe the hydrodynamic effect of spherical particles in the fluid and was later introduced to the

field of filled elastomers by Smallwood in 1944.<sup>54,55</sup> The equation requires freely dispersed solid spherical particle inside the rubbery matrix, and the constant 2.5 is a geometry factor that works for spherical particles. Based on the Smallwood equation, the Guth model also takes the interactions between particle pairs into consideration, as shown in the following Smallwood-Guth-Einstein equation:<sup>56</sup>

$$G = G_m(1 + 2.5\phi + 14.1\phi^2)$$

To further understand how the mechanical properties of elastomers are enhanced by the addition of fillers, the factor to be considered is the size of the filler particles. As shown in Figure 1.6, fillers with particle size larger than  $10^3$  nm usually have very limited reinforcing capabilities which is mainly the weak hydrodynamic effect. However such fillers are still important in industry since they can largely reduce the cost of the final product. The reinforcing capabilities of fillers increases as the particle size becomes smaller, and the most efficient fillers commonly have particle size lower than  $10^2$  nm. Within this range, the influence of primary particle size is no longer the primary importance since the fillers in the polymer matrix will not present as independent particles but aggregates. So other parameters such as the primary particle shape and their aggregate structure become more decisive., and the filler-filler interaction and polymer-filler interaction are two most important factors that have strong influence on the reinforcing effect of the filler aggregates.<sup>57</sup> Both filler-filler interaction and polymer-filler interaction happen on the surface of filler aggregates, these two interactions depends largely on the filler aggregate morphology and the filler surface activity.

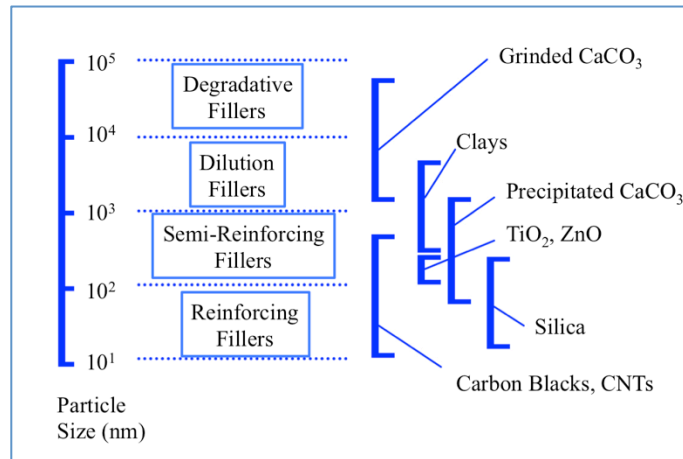


**Figure 1.6**

Relationship between filler's reinforcement effect and particle size.<sup>57</sup>

Filler-filler interaction mainly refers to the interaction between filler particles/aggregates that will form into the filler-filler network. At low filler loading, since the volume fraction of filler is low compared to that of polymer, filler-filler interaction is weak as long as filler is well dispersed into the polymer matrix. However at high filler loading, filler-filler interaction becomes important, because it will lead to the formation of larger agglomerates by the combining of several filler aggregates together. The reinforcing effect caused by filler-filler interaction occurs at low strain level. This is described as the Payne effect, for which the shear modulus undergoes a decrease starting from low strain, due to the breakdown of filler-filler network (Figure 1.7). At higher strain, the filler-filler network is totally broken down and will not contribute to the material's mechanical property.

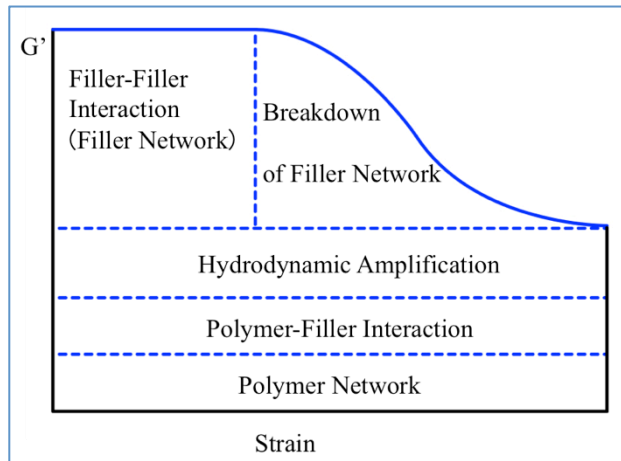


**Figure 1.7**

Different contributions to the modulus of elastomers.

Polymer-filler interaction involves the interfacial van der Waals force between polymer chains and filler particles/aggregates, as well as hydrogen bonds or covalent bonds that form between polymers and fillers. By “connection” of polymer chains and filler particles, a secondary network between filler and polymer is created that alters the mechanical properties of elastomers. In conclusion, at higher strains the main contribution of filler to the material’s mechanical property is polymer-filler interaction and hydrodynamic reinforcement, while at low strain, filler-filler interaction should also be considered. These three factors, together with the polymer network itself, determine the mechanical properties of an elastomer (Figure 1.7).

### 1.3.2 Carbon Black Filler

Carbon black is one of the first studied reinforcing agent for elastomers and is still extensively used in industry today. Typical carbon black consists of spherical particles that range from 5-100 nm in size and can aggregate into 100 to 500 nm structures.<sup>58</sup> Mechanical, electrical and optical properties of elastomers can be enhanced upon with the addition of carbon black fillers due to the rigid, conductive and UV protective nature of carbon black.<sup>59-61</sup>

Different types of carbon black have different aggregate morphologies such as spherical structure and highly branched structure, depending on the way they are manufactured.<sup>57</sup> The aggregate morphology of carbon black plays an important role in determining its reinforcing effect. In general, carbon black aggregate with more complex branched structures (higher surface area) can be better dispersed into polymer compared with carbon black that has more simple structures (lower surface area). A better dispersion benefits the polymer-filler interaction and thus will lead to better mechanical properties. However, carbon black with highly branched structure also has more voids containing air inside that is hard to remove.<sup>58</sup> So the preparation of elastomer with highly branched carbon black will be challenging because trapped air in the elastomer serves as structural defects that will reduce the tensile strength and modulus of the elastomer.

Carbon black has also been reported to enhance the mechanical properties of polyolefin-based elastomers. For example, Baer et al. studied the mechanical properties of carbon black filled ethylene-octene (EO) elastomer as a function of filler content.<sup>62</sup> The stress-strain behavior of the filled EO demonstrated a gradual improvement in the

modulus and tensile strength with increasing filler volume fraction. The elongation at break of the filled EO remained at a constant level and the commonly observed decrease in the break elongation upon with the addition of the carbon black filler was not observed in their research. The reinforcing effect was also compared with the prediction of hydrodynamic effect using the classical Guth model, and a significant difference was observed even under a lower filler volume fraction (10%), indicating that other parameters such as the morphology of fillers, filler-filler interaction have to be considered when describing the reinforcing effect of the carbon black filler.

### **1.3.3 Silica Filler**

Besides the widely used carbon black filler, silica particle with outstanding chemical inertness and durability is widely recognized as an effective filler and is now extensively used and studied.<sup>58,63,64</sup> However, since the siloxane and silanol groups on the surface of silica particles are hydrophilic in nature, the interaction between the hydrophilic silica surface and hydrophobic polymer backbones are relatively weak. On the other hand, the filler-filler interaction is strong due to the hydrogen bonds between silica particles. Also, silica particles or aggregates tend to form into larger agglomerates that will lead to inhomogeneous filler distribution, which makes the dispersion of silica particles more difficult than that of carbon black.<sup>58,65</sup>

In terms of polyolefin based elastomers, silica fillers have been reported to be able enhance their mechanical properties.<sup>62,66-68</sup> For example, Morselli et al. studied a series of silica filled EPDM rubber and found that the modulus of a sample with 30 wt% of silica filler was 2.5 times higher than the unfilled sample, while the elongation at break for the

filled sample was about 2 times higher than the unfilled one.<sup>66</sup> The initial modulus of the filled EPDM was also compared with the prediction of the Guth equation and the experimental modulus values were significantly higher than the predicted values under high filler loadings, and the observed difference was related to the formation of filler aggregates under high filler loading that lead to additional “crosslinks” in the polymer matrix. The dynamic mechanical analysis agreed with the tensile measurement that the storage modulus of the filled sample increased significantly, while the glass transition temperature for the filled sample was about the same compared to the unfilled one. Thermal stability study by TGA showed very similar thermal degradation behavior for the filled and the unfilled EPDM, suggesting that the thermal stability enhancement by the presence of the filler was negligible.

To better disperse silica particles in polymer and reduce the size and amount of silica agglomerates, one effective solution is to modify the surface of silica particles with silane coupling agents.<sup>69-71</sup> Bis(3-(triethoxysilyl)-propyl)tetrasulfide (TESPT) is one commonly used silane coupling agent that can modify the surface of silica particles and better disperse them into polyethylene-based polymers or other polymers with carbon-carbon backbone.<sup>72,73</sup> For example, Qu et al. studied the effect of TESPT modified silica on mechanical property of styrene butadiene rubber, and the tensile property was found to be related with TESPT loading.<sup>74</sup> With high TESPT loading, the tensile strength and modulus were all improved while the elongation at break value was reduced. They also observed that without TESPT treatment, silica formed into large agglomerates in the sample, while TESPT modified silica particles were well dispersed according to TEM.

Figure 1.8 shows the treatment of silica particle using TESPT, in which the silanol groups on the surface of silica particle react with the ethoxy group by condensation. Hydrogen bonds between silica particles will be largely reduced after the modification and the filler-filler interaction will be weakened.

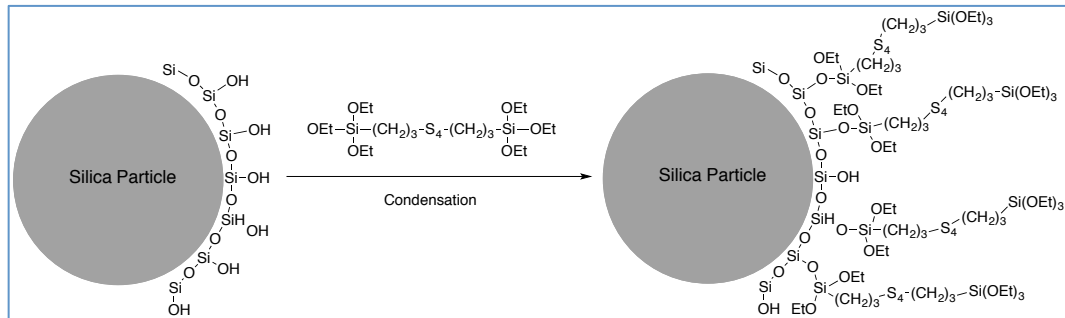


**Figure 1.8**

Surface treatment of the hydrophilic silica particle with TESPT.<sup>51</sup>

Another advantage of TESPT modified silica is that the sulfur bond in TESPT can insert into unsaturated carbon-carbon bonds along the polymer backbone. Mixing such polymers with unsaturated carbon-carbons with TESPT modified silica particles will result in the formation of chemical bond between fillers and prepolymers. This will benefit the dispersion of silica filler and enhance the polymer-filler interaction.



## **1.4 Conclusions**

The synthesis of telechelic polyolefin prepolymers with functional end-groups via ring-opening metathesis polymerization with chain transfer agent is briefly discussed in the first part of this chapter. Since the synthesized elastomers from the crosslinking of the prepolymers with tri-functional crosslinkers are weak in their mechanical behaviors, the use of reinforcing fillers such as carbon black and silica as an effective solution to enhance the mechanical properties of elastomers are summarized in the second part of this section.

## 1.5 References

- (1) Hiemenz, P. C.; Lodge, T. *Polymer chemistry*; 2nd ed.; CRC Press: Boca Raton, 2007.
- (2) Sommer, J. G.; Knoel (Firm); Hanser,; Munich ; Cincinnati, 2009, p ix.
- (3) Mark, J. E.; Eriman, B.; Eirich, F. R.; 3rd ed.; Elsevier Academic Press,; Amsterdam ; Boston, 2005, p 1 online resource.
- (4) Hild, G. *Progress in Polymer Science* **1998**, *23*, 1019.
- (5) Bontems, S. L.; Stein, J.; Zumburum, M. A. *J Polym Sci Pol Chem* **1993**, *31*, 2697.
- (6) Delebecq, E.; Ganachaud, F. *Acs Appl Mater Inter* **2012**, *4*, 3340.
- (7) Delebecq, E.; Hermeline, N.; Flers, A.; Ganachaud, F. *Acs Appl Mater Inter* **2012**, *4*, 7075.
- (8) Biswas, A.; Bandyopadhyay, A.; Singha, N. K.; Bhowmick, A. K. *J Mater Sci* **2009**, *44*, 3125.
- (9) Tasdelen, M. A.; Kahveci, M. U.; Yagci, Y. *Progress in Polymer Science* **2011**, *36*, 455.
- (10) Grubbs, R. H. *Handbook of metathesis*; Wiley-VCH: Weinheim, Germany, 2003.
- (11) Martinez, H.; Miro, P.; Charbonneau, P.; Hillmyer, M. A.; Cramer, C. J. *Acs Catal* **2012**, *2*, 2547.
- (12) Bielawski, C. W.; Grubbs, R. H. *Progress in Polymer Science* **2007**, *32*, 1.
- (13) Katz, T. J.; Lee, S. J.; Acton, N. *Tetrahedron Lett.* **1976**, 4247.
- (14) Schrock, R. R. *J Organomet Chem* **1986**, *300*, 249.
- (15) Schrock, R. R. *Accounts Chem Res* **1990**, *23*, 158.

- (16) Preishuber-Pflugl, P.; Buchacher, P.; Eder, E.; Schitter, R. M.; Stelzer, F. *J Mol Catal a-Chem* **1998**, *133*, 151.
- (17) Flook, M. M.; Jiang, A. J.; Schrock, R. R.; Muller, P.; Hoveyda, A. H. *J Am Chem Soc* **2009**, *131*, 7962.
- (18) Dounis, P.; Feast, W. J.; Kenwright, A. M. *Polymer* **1995**, *36*, 2787.
- (19) Chung, T. C. *J Mol Catal* **1992**, *76*, 15.
- (20) Demonceau, A.; Noels, A. F.; Saive, E.; Hubert, A. J. *J Mol Catal* **1992**, *76*, 123.
- (21) Nguyen, S. T.; Grubbs, R. H.; Ziller, J. W. *J Am Chem Soc* **1993**, *115*, 9858.
- (22) Schwab, P.; Grubbs, R. H.; Ziller, J. W. *J Am Chem Soc* **1996**, *118*, 100.
- (23) Bielawski, C. W.; Grubbs, R. H. *Angew Chem Int Edit* **2000**, *39*, 2903.
- (24) Kingsbury, J. S.; Harrity, J. P. A.; Bonitatebus, P. J.; Hoveyda, A. H. *J Am Chem Soc* **1999**, *121*, 791.
- (25) Love, J. A.; Morgan, J. P.; Trnka, T. M.; Grubbs, R. H. *Angewandte Chemie-International Edition* **2002**, *41*, 4035.
- (26) Garber, S. B.; Kingsbury, J. S.; Gray, B. L.; Hoveyda, A. H. *J Am Chem Soc* **2000**, *122*, 8168.
- (27) P'pool, S. J.; Schanz, H. J. *J Am Chem Soc* **2007**, *129*, 14200.
- (28) Dunbar, M. A.; Balof, S. L.; LaBeaud, L. J.; Yu, B.; Lowe, A. B.; Valente, E. J.; Schanz, H. J. *Chem-Eur J* **2009**, *15*, 12435.
- (29) Demonceau, A.; Stumpf, A. W.; Saive, E.; Noels, A. F. *Macromolecules* **1997**, *30*, 3127.

- (30) Monsaert, S.; Ledoux, N.; Drozdak, R.; Verpoort, F. *J Polym Sci Pol Chem* **2010**, *48*, 302.
- (31) Ledoux, N.; Allaert, B.; Schaubroeck, D.; Monsaert, S.; Drozdak, R.; Van Der Voort, P.; Verpoort, F. *J Organomet Chem* **2006**, *691*, 5482.
- (32) Vougioukalakis, G. C.; Grubbs, R. H. *Chem-Eur J* **2008**, *14*, 7545.
- (33) Allaert, B.; Dieltiens, N.; Ledoux, N.; Vercaemst, C.; Van der Voort, P.; Stevens, C. V.; Linden, A.; Verpoort, F. *J Mol Catal a-Chem* **2006**, *260*, 221.
- (34) Vougioukalakis, G. C.; Grubbs, R. H. *J Am Chem Soc* **2008**, *130*, 2234.
- (35) Ivin, K. J.; Mol, J. C. *Olefin metathesis and metathesis polymerization*; Academic Press: San Diego, 1997.
- (36) Maughon, B. R.; Morita, T.; Bielawski, C. W.; Grubbs, R. H. *Macromolecules* **2000**, *33*, 1929.
- (37) Morita, T.; Maughon, B. R.; Bielawski, C. W.; Grubbs, R. H. *Macromolecules* **2000**, *33*, 6621.
- (38) Pitet, L. M.; Hillmyer, M. A. *Macromolecules* **2011**, *44*, 2378.
- (39) Ji, S. X.; Hoye, T. R.; Macosko, C. W. *Macromolecules* **2004**, *37*, 5485.
- (40) Hillmyer, M. A.; Grubbs, R. H. *Macromolecules* **1993**, *26*, 872.
- (41) Hillmyer, M. A.; Grubbs, R. H. *Macromolecules* **1995**, *28*, 8662.
- (42) Hillmyer, M. A.; Nguyen, S. T.; Grubbs, R. H. *Macromolecules* **1997**, *30*, 718.
- (43) Pitet, L. M.; Hillmyer, M. A. *Macromolecules* **2009**, *42*, 3674.
- (44) Kobayashi, S.; Kim, H.; Macosko, C. W.; Hillmyer, M. A. *Polym Chem-Uk* **2013**, *4*, 1193.

- (45) Bielawski, C. W.; Morita, T.; Grubbs, R. H. *Macromolecules* **2000**, *33*, 678.
- (46) Mahanthappa, M. K.; Bates, F. S.; Hillmyer, M. A. *Macromolecules* **2005**, *38*, 7890.
- (47) Sill, K.; Emrick, T. *J Polym Sci Pol Chem* **2005**, *43*, 5429.
- (48) Kobayashi, S.; Macosko, C. W.; Hillmyer, M. A. *Aust J Chem* **2010**, *63*, 1201.
- (49) Kobayashi, S.; Pitet, L. M.; Hillmyer, M. A. *J Am Chem Soc* **2011**, *133*, 5794.
- (50) Martinez, H.; Hillmyer, M. A. *Macromolecules* **2014**, *47*, 479.
- (51) Wypych, G.; Knovel (Firm); [3rd ed.; ChemTec Pub.,: Toronto, 2010, p xx.
- (52) Moniruzzaman, M.; Winey, K. I. *Macromolecules* **2006**, *39*, 5194.
- (53) Kuilla, T.; Bhadra, S.; Yao, D. H.; Kim, N. H.; Bose, S.; Lee, J. H. *Prog Polym Sci* **2010**, *35*, 1350.
- (54) Einstein, A. *Annalen der Physik* **1906**, *324*, 289.
- (55) Smallwood, H. M. *Journal of Applied Physics* **1944**, *15*, 758.
- (56) Guth, E. *Journal of Applied Physics* **1945**, *16*, 20.
- (57) Leblanc, J. L. *Progress in Polymer Science* **2002**, *27*, 627.
- (58) Vilgis, T. A.; Heinrich, G.; Klüppel, M. *Reinforcement of polymer nanocomposites : theory, experiments and applications*; Cambridge University Press: Cambridge, UK ; New York, 2009.
- (59) Huang, J. C. *Adv Polym Tech* **2002**, *21*, 299.
- (60) Zhang, A. Q.; Wang, L. S.; Lin, Y. L.; Mi, X. F. *J Appl Polym Sci* **2006**, *101*, 1763.
- (61) Santos, R. M.; Botelho, G. L.; Machado, A. V. *J Mater Sci* **2014**, *49*, 510.

- (62) Flandin, L.; Hiltner, A.; Baer, E. *Polymer* **2001**, *42*, 827.
- (63) Aranguren, M. I.; Mora, E.; Macosko, C. W. *J Colloid Interf Sci* **1997**, *195*, 329.
- (64) Dorigato, A.; Pegoretti, A.; Fambri, L.; Slouf, M.; Kolarik, J. *J Appl Polym Sci* **2011**, *119*, 3393.
- (65) Kato, A.; Ikeda, Y.; Tsushi, R.; Kokubo, Y. *J Appl Polym Sci* **2013**, *130*, 2594.
- (66) Morselli, D.; Bondioli, F.; Luyt, A. S.; Mokhothu, T. H.; Messori, M. *J Appl Polym Sci* **2013**, *128*, 2525.
- (67) Abou-Kandil, A. I.; Gaafar, M. S. *J Appl Polym Sci* **2010**, *117*, 1502.
- (68) Lv, X. F.; Zhang, B. S.; Qiu, G. X. *J Appl Polym Sci* **2012**, *125*, 3794.
- (69) Scotti, R.; Wahba, L.; Crippa, M.; D'Arienzo, M.; Donetti, R.; Santo, N.; Morazzoni, F. *Soft Matter* **2012**, *8*, 2131.
- (70) Joseph, R.; Alex, R.; Madhusoodanan, K. N.; Premalatha, C. K.; Kuriakose, B. *J Appl Polym Sci* **2004**, *92*, 3531.
- (71) Sun, Y. Y.; Zhang, Z. Q.; Wong, C. P. *J Colloid Interf Sci* **2005**, *292*, 436.
- (72) Wang, R. G.; Yao, H.; Lei, W. W.; Zhou, X. X.; Zhang, L. Q.; Hua, K. C.; Kulig, J. *J Appl Polym Sci* **2013**, *129*, 1546.
- (73) Saeed, F.; Ansarifar, A.; Ellis, R. J.; Haile-Meskel, Y.; Irfan, M. S. *J Appl Polym Sci* **2012**, *123*, 1518.
- (74) Qu, L. L.; Yu, G. Z.; Xie, X. M.; Wang, L. L.; Li, J.; Zhao, Q. S. *Polym Composite* **2013**, *34*, 1575.

# Chapter 2

## Synthesis of Polyolefin Elastomers via a ROMP-Hydrogenation-Crosslinking Method and the Reinforcement of the Elastomers with Fillers

Telechelic polyolefin with carboxylic end groups was synthesized by ROMP of 3-ethyl-1-cyclooctene with maleic acid as CTA. The telechelic polymer was then hydrogenated to obtain saturated telechelic polyethylene that can be further crosslinked to elastomers. Carbon black and fumed silica were used as fillers to reinforce the polyethylene elastomers and their mechanical properties were studied.

## 2.1. Introduction

Liquid Silicon Rubbers (LSR), like crosslinked polydimethylsiloxane (PDMS), are a class of amorphous polymers with glass transition temperatures ( $T_g$ ) as low as – 123 °C.<sup>1</sup> Two component LSRs, containing PDMS containing vinyl groups and PDMS with backbone silane groups, can be crosslinked to prepare silicon elastomers. For example, telechelic  $\alpha,\omega$ -divinyl polydimethylsiloxane can be obtained by the anionic polymerization of cyclic siloxane,<sup>5</sup> the vinyl end groups can then react with silicone polymers that have multiple Si-H groups. LSRs have excellent hydrophobicity, a wide operating temperature range, and a high elongation at break and therefore have a wide range of applications, including sealing and joint applications.<sup>6,75</sup>

Previously we synthesized a telechelic polyolefin prepolymer with carboxylic end-groups and this prepolymer was further crosslinked into a polyolefin elastomer with LSR-like properties.<sup>50</sup> To achieve this we first synthesized an unsaturated telechelic polymer by ring-opening metathesis polymerization (ROMP) of alkyl substituted cyclooctene derivatives with a di-functional chain transfer agent (CTA) to control the molar mass and end-group functionality.<sup>23,44,48,76,77</sup> The unsaturated polymer synthesized by ROMP was hydrogenated to obtain saturated polyolefin prepolymer and the prepolymer was then crosslinked by the tri-functional crosslinker tris-aziridine (Taz) to obtain elastomers. However, compared with commercially available LSR, the uniaxial tensile properties of the polyethylene elastomers were not at the level of typical LSRs. To further enhance the performance of the elastomers, carbon black filler and silica filler were used for the mechanical properties reinforcement.



In the present work we report a (i) a modified and simplified synthesis of carboxy-telechelic polyolefin prepolymers based on our previous work and (ii) a straightforward approach to significantly enhance the mechanical properties of the materials through the addition of fumed silica and carbon black fillers (Figure 2.1). To further understand the reinforcing mechanism, the thermal, mechanical and rheological properties of the filled elastomers are carefully studied.

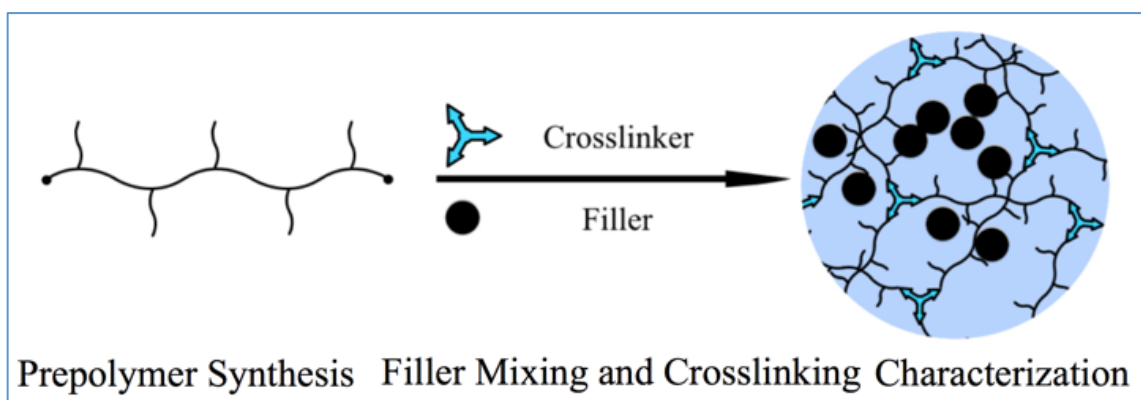
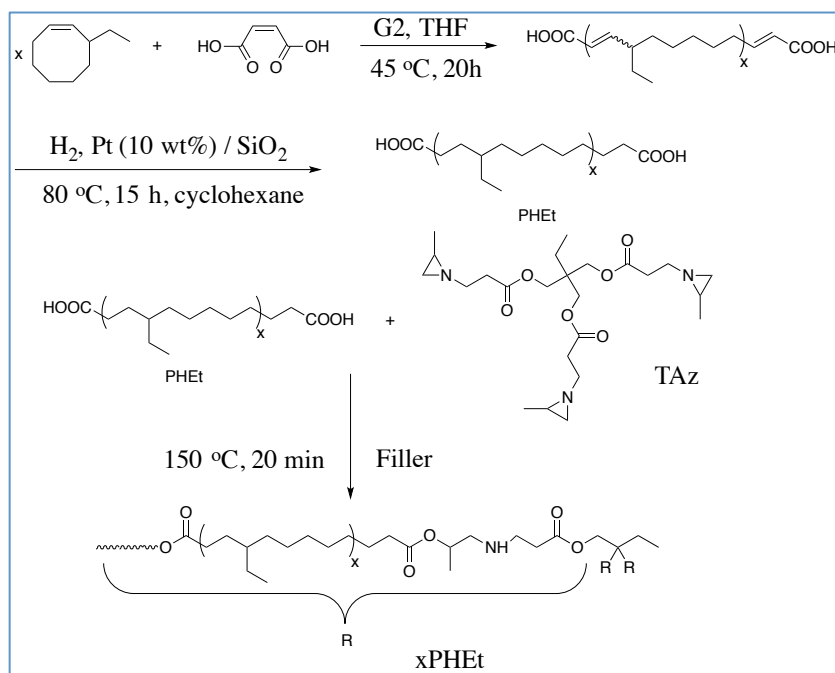


**Figure 2.1**  
Filler reinforced elastomers from telechelic polyolefin prepolymers.

## 2.2 Results and Discussion

### 2.2.1 Prepolymer Synthesis

Scheme 2.1 shows the synthetic route for the carboxy-telechelic prepolymers by homopolymerization of 3-ethyl-1-cyclooctene, followed by hydrogenation. Similar to our previous report, maleic acid was used as CTA to control the molar mass and install carboxylic acid end groups.<sup>50</sup> The target molar mass was 4 kg/mol to keep the viscosity of the prepolymer low and provide a high crosslink density (i.e., a high concentration of crosslinkable end-groups). The prepolymer was hydrogenated using a SiO<sub>2</sub> supported platinum catalyst. The obtained saturated prepolymer (PHEt) is amorphous with  $T_g \approx -70$  °C. Compared to our previous report, in which the prepolymer was obtained by copolymerization of cis-cyclooctene and 3-hexyl-1-cyclooctene, the homopolymerization of 3-ethyl-1-cyclooctene is a more straightforward reaction (i.e., a homopolymerization) that leads to a more regular polymer chain structure with a lower  $T_g$  than our previously synthesized polymers. <sup>1</sup>H NMR characterization of the prepolymer before and after hydrogenation suggests that the CTA was successfully incorporated into the prepolymer and over 98% of the unsaturated double bond were hydrogenated (Figure 2.2). The molar mass of the prepolymer was calculated to be 4.3 kg/mol using <sup>1</sup>H NMR spectroscopy, assuming that each chain has exactly two end-groups.



**Scheme 2.1**

Synthesis of carboxy-telechelic prepolymer via ROMP followed by hydrogenation and crosslinking of hydrogenated prepolymer using TAz.

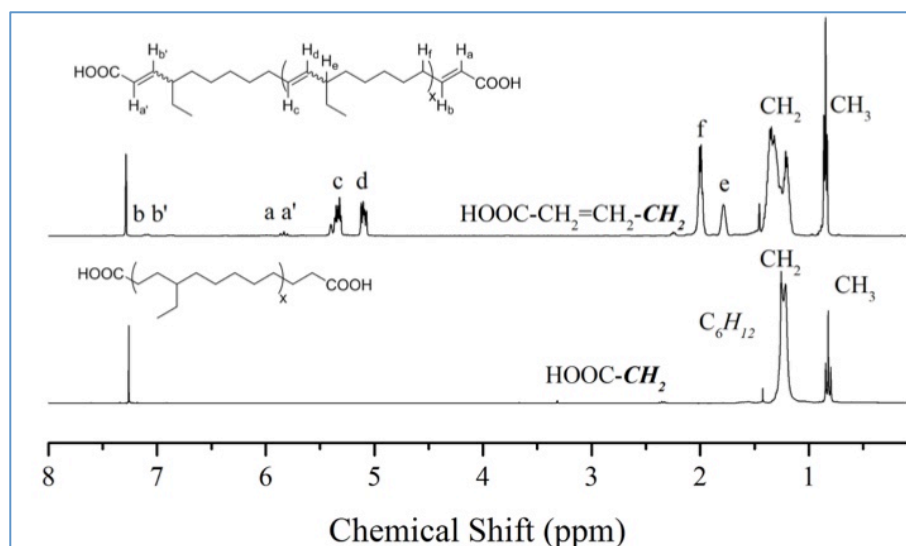


**Figure 2.2**

<sup>1</sup>H NMR characterization of the prepolymer before and after hydrogenation.

### 2.2.2 Filler Incorporation and crosslinking of prepolymers

Two types of fillers, Aerosil R-812 (hydrophobic silica, surface area 260 m<sup>2</sup>/g, produced by Evonik) and V7H (low structure carbon black, surface area 112 m<sup>2</sup>/g, produced by Cabot) were used in this experiment. The silica filler used in this experiment is typically named “fumed silica” since it is obtained from the reaction between silica tetrachloride and water by a vapor process under 1800 °C that seems like fumes.<sup>78</sup>

To prepare the filled elastomer, the prepolymer was first mechanically mixed with different amount of filler to prepare mixtures that contained 5, 10, 20, and 30 wt% of fumed silica/carbon black filler. The mixtures were further homogenized with a speed-mixer at 2800 rpm for 30 min to ensure that filler particles were well dispersed into the polymer matrix. Viscosities of the mixtures increased dramatically with the addition of filler, indicating that the processing of the mixture and the dispersion of filler became more difficult with increasing filler content. After the initial mixing, the tri-functional crosslinker was then added into the well-mixed prepolymer-filler mixture (with 3:2 prepolymer : crosslinker mole ratio), and a speed-mixer was used again to mix the tris-aziridine into the prepolymer. The ternary mixtures of prepolymer, tris-aziridine and filler were then molded into a rectangular films (8.3 cm × 8.3 cm × 1 mm, ≈ 6.7 g) at 150 °C and 3000 psig for 20 min (Scheme 2.1). After press-molding, samples were left to cure in oven at 100 °C for 6 h to drive the crosslinking reaction to completion. (Half time for this crosslinking reaction was calculated to be 531s at 100 °C according to our previous study.<sup>50</sup>)

The critical extent of reaction ( $P_c$ ) is calculated to be 0.71 for this crosslinking reaction.<sup>1</sup> Further gel fraction test for the crosslinked elastomers demonstrates that the gel fraction for all the samples are higher than 90%, indicating that the prepolymers are well crosslinked by the tris-aziridine. Samples with silica particles are transparent while samples with carbon black are black.

### **2.2.3 Morphology Study**

Scanning electron microscope (HIACHI 4700 FE-SEM) was used to study the morphology of the fillers and the polyolefin elastomers with fillers. As shown in Figure 2.3a and 2.3b, the scans under low resolution (1K) suggest that both silica filler and carbon black filler do not present in the form of primary particles but the aggregates. The aggregate of silica filler demonstrates a larger size distribution when compared to the aggregate of carbon black filler. In general the size of fumed silica aggregates ranges from 2  $\mu\text{m}$  to 15  $\mu\text{m}$  while the size of V7H carbon black aggregates ranges from 2  $\mu\text{m}$  to 8  $\mu\text{m}$ . The scans under higher resolution (Figure 2.3c and 2.3d) reveals that there exist fine silica particles around the silica aggregate while carbon black aggregate has a more compact structure. The silica particles around the aggregate may become part of the aggregate after the filler is mixed with the polyethylene prepolymer, since the interaction between silica particles will be stronger than the interaction between the silica and polyethylene chain.

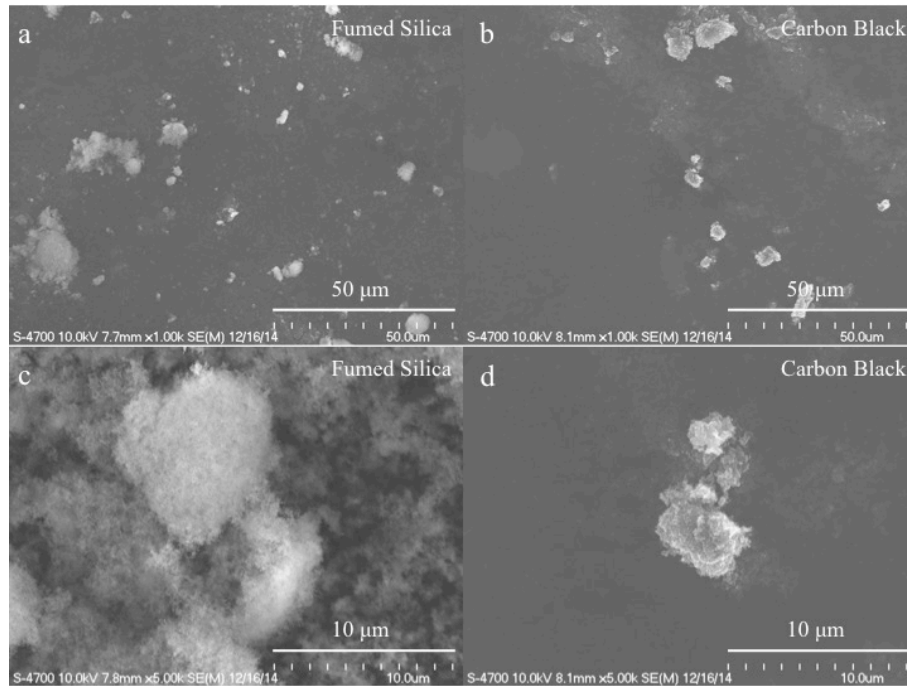


**Figure 2.3**

Representative SEM images of fumed silica and carbon black fillers.

For polyethylene samples with the carbon black filler (Figure 2.4), the size of filler-filler aggregates increases with filler content; at 5 wt% filler content, the carbon black filler are well separated and there is no filler-filler network, when the filler goes to 30 wt%, large aggregates can be observed, which is evidence for a filler network. For the fumed silica filled samples (Figure 2.5), however, large aggregates appear in samples with 10 wt% of filler. This is another evidence that the fine silica particles will further participate in the silica aggregate in the polymer matrix since the filler-filler interaction is much stronger than the polymer-filler interaction in this case. Therefore, the fumed silica filler can form into filler-filler networks easier (at lower filler content) than the carbon black filler.

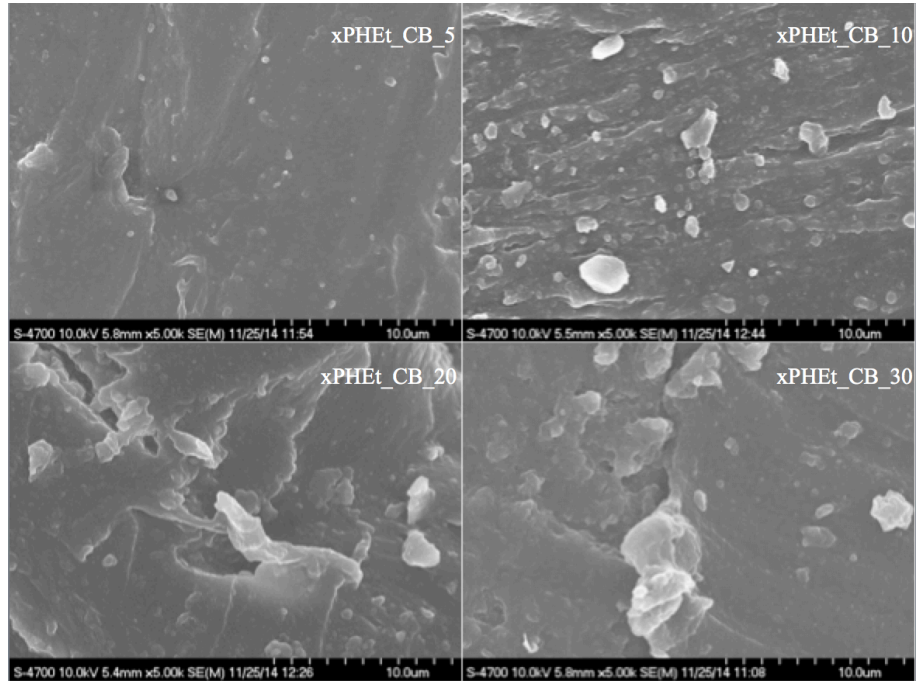


**Figure 2.4.**  
SEM images of carbon black filled polyolefin elastomers.

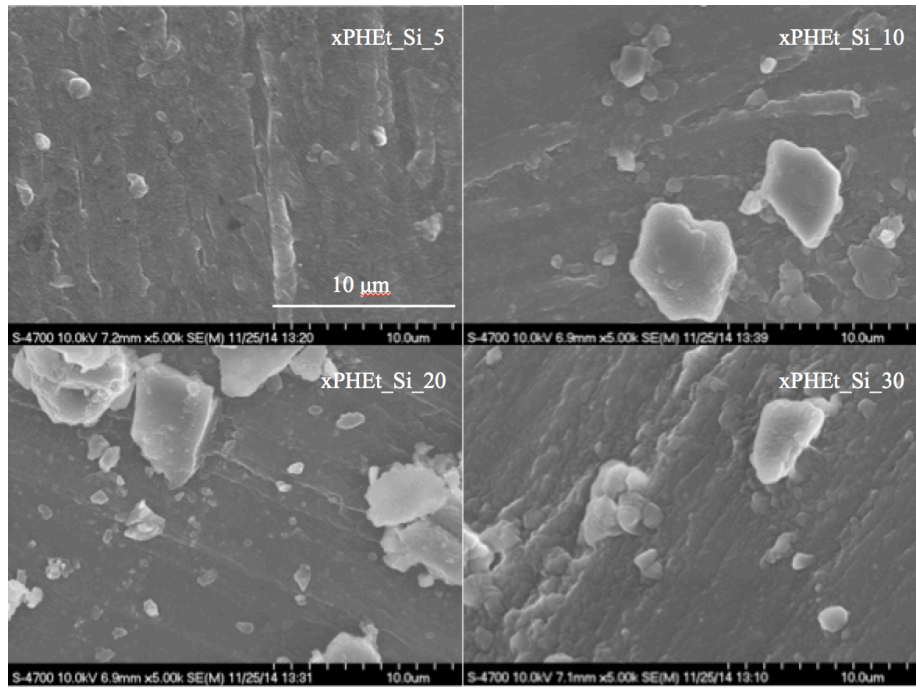


**Figure 2.5**  
SEM images of fumed silica filled polyolefin elastomers.

#### 2.2.4 Thermal Properties

The  $T_g$  values for both fumed silica and carbon black filled samples are essentially the same as for the unfilled and crosslinked samples, suggesting that the interactions between the polyethylene prepolymer and the fillers are not enough to significantly raise the glass transition temperature even at high level of filler loading. The degradation temperature (at 5% weight loss,  $T_d$ ) of the filled elastomers increases with the addition of the filler. Although the shift in  $T_d$  suggests an enhancement in the thermal stability of the filled elastomer,<sup>64,79</sup> this enhancement is due to the fact that both type of fillers will not degrade during the thermal gravimetric analysis experiment, and the weight loss was mainly caused by the degradation of the polymer.



**Table 2.1**

Filler content and thermal properties of filled elastomers.

Sample ID	Filler Type	Filler Content (wt %)	$T_g$ (°C) <sup>a</sup>	$T_d$ (°C) <sup>b</sup>
xPHEt			-68	317
xPHEt-Si5	Aerosil R-812	5	-68	344
xPHEt-Si10	Aerosil R-812	10	-68	360
xPHEt-Si20	Aerosil R-812	20	-70	369
xPHEt-Si30	Aerosil R-812	30	-71	375
xPHEt-CB5	V7H	5	-69	357
xPHEt-CB10	V7H	10	-70	356
xPHEt-CB20	V7H	20	-67	356
xPHEt-CB30	V7H	30	-70	375

<sup>a</sup> Determined by DSC (second heating cycle) at 10 °C min<sup>-1</sup>. <sup>b</sup> 5% weight loss determined by TGA at 10 °C min<sup>-1</sup> in N<sub>2</sub>.

## 2.2.5 Rheological Properties

### 2.2.5.1 Viscosity

Before crosslinking, the viscosity of the prepolymer-filler mixture was first studied. The viscosity of the filler-prepolymer mixture is an important parameter because a higher viscosity suggests that the processing of the mixture is much more difficult and needs extra energy. As shown in Figure 2.6, the viscosity of the prepolymer-filler mixture increases significantly with fillers. For prepolymers with no filler, the viscosity is only about 100 Pa·s while the viscosity of the prepolymer with 30 wt% of fillers was higher than 1 MPa·s. This is about 10000 times higher so it was impossible to achieve the Newtonian behavior at the lower limit of the instrument. Compared with the commercially available LSR before crosslinking, viscosity of prepolymer-filler mixture is slightly higher than that of LSR, this is consistent with the higher shear modulus of the filled elastomers (Figure 2.7).

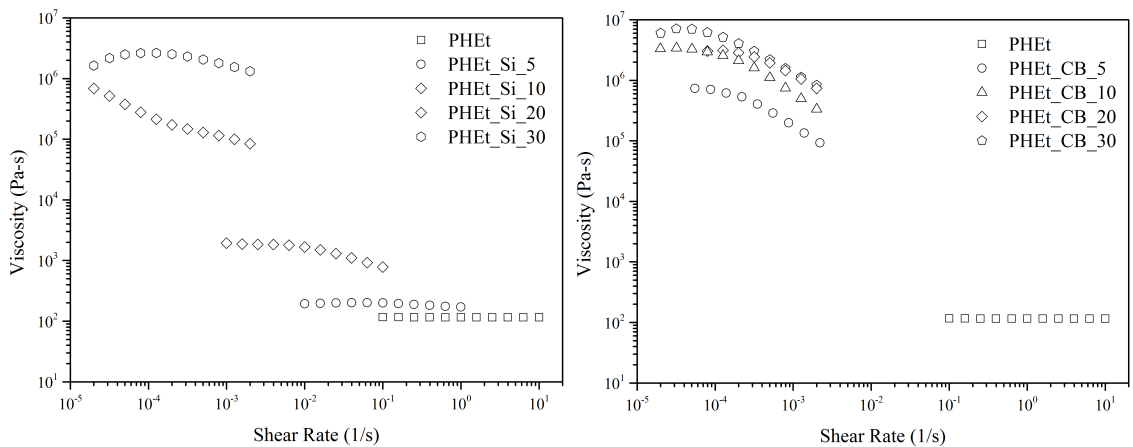


**Figure 2.6.**  
Viscosity of prepolymer-filler mixture.

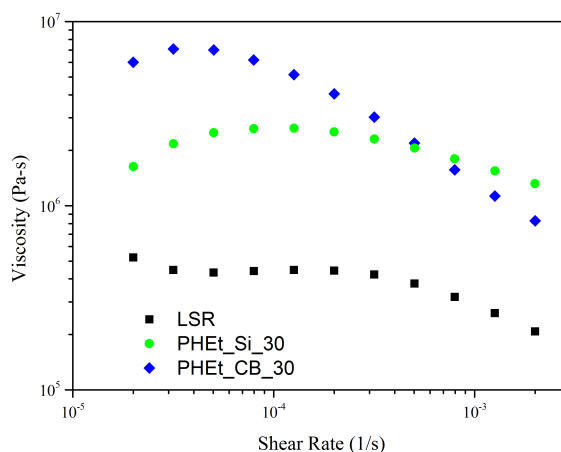


**Figure 2.7.**

Viscosity of prepolymer-filler mixture and LSR before crosslinking.

### 2.2.5.2 Dynamic Mechanical Thermal Analysis

To better understand the mechanical behavior of the filled elastomers and the polymer-filler interaction, dynamic mechanical thermal analysis was performed on all the samples over wide temperature range. Figure 2.8 and Figure 2.9 show the temperature-storage modulus relationship of filled elastomers from -90 °C to 200 °C under 6.28 Hz. At temperatures lower than -70 °C, the samples are at their glassy state with a  $G'$  between 500 MPa and 2 GPa. With increasing temperature, their storage modulus drop significantly for about 2 decades after passing  $T_g$ . Above -50 °C they are already at their rubbery plateau and their storage modulus of the crosslinked samples remains at a quite constant level.

For both silica and carbon black filled elastomers, their storage modulus at the rubbery plateau become higher with increasing amount of filler, which is consistent with the initial elastic modulus obtained by tensile testing. The addition of filler has little influence on the glass transition temperature of the elastomer, which agrees with the DSC experiment.

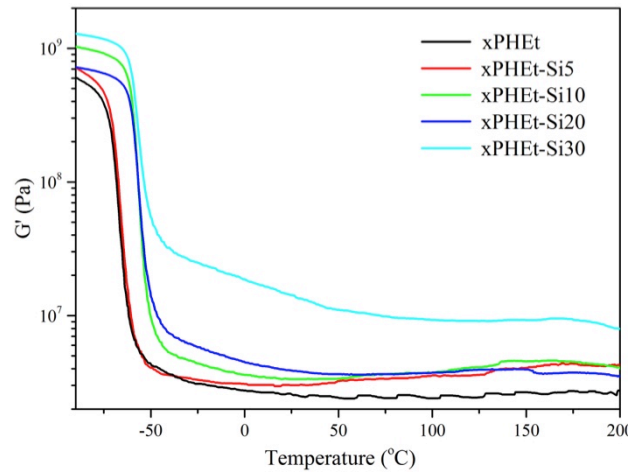


**Figure 2.8**  
Dynamic mechanical thermal analysis of silica filled elastomers.

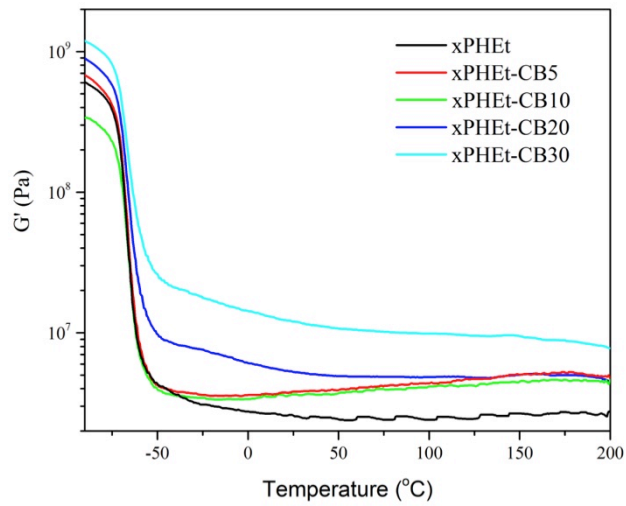


**Figure 2.9**  
Dynamic mechanical thermal analysis of carbon black filled elastomers.

### 2.2.5.3 Frequency Sweep at Room Temperature

The storage moduli of the prepolymers under different shear frequency at room temperature were also measured to study the behavior of the elastomers (Figure 2.10). While the samples present a low frequency dependence, it decreases as filler amount increases, this is consistent with previous reports, suggesting that the existence of filler-polymer interaction influences the movement of the chain segment on the surface of the filler aggregates.<sup>80,81</sup> Both samples with fumed silica and carbon black have a higher storage modulus than LSR at room temperature (Figure 2.11), which suggests that for the silicon elastomer, the apparent molar mass between crosslinks is higher compared to our materials.

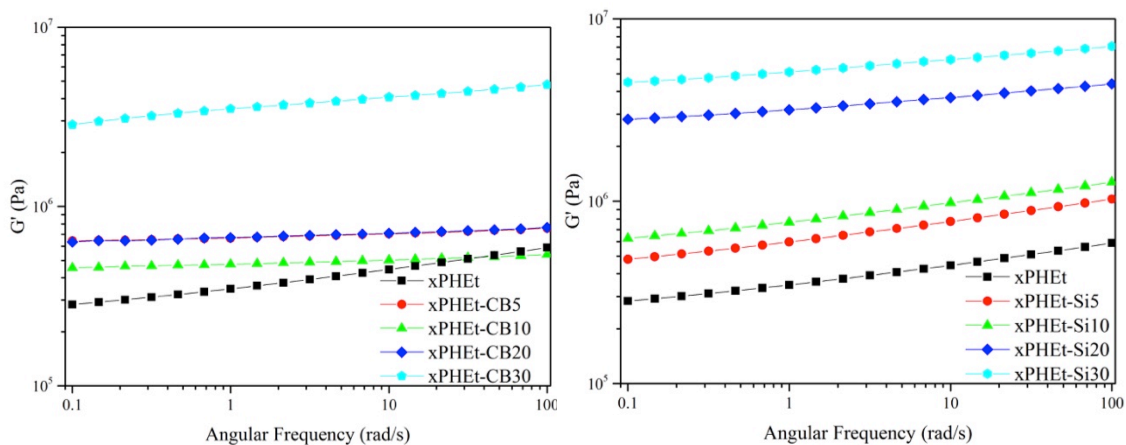


**Figure 2.10**

Frequency sweep (25 °C) of crosslinked PHEt with fillers.

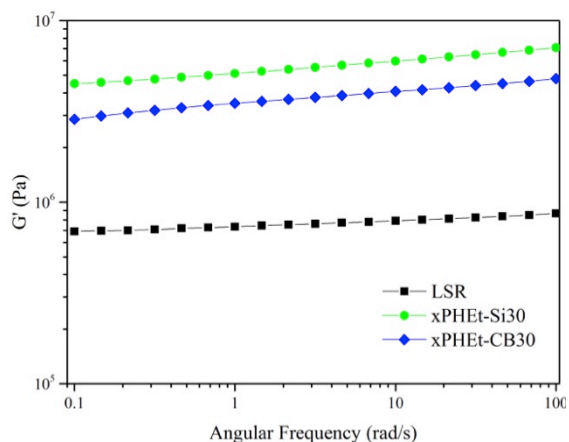


**Figure 2.11**

Frequency sweep (25 °C) of crosslinked elastomers and LSR.

#### 2.2.5.4 Payne Effect

One well-known behavior of a filled elastomer with filler-filler interaction is the Payne effect, which is the drop in modulus with a small strain increase.<sup>82,83</sup> This is clearly observed in the silica filled elastomers. Figure 2.12 (left) shows the room temperature oscillation sweep study on the fumed silica reinforced elastomers. For the sample with no filler reinforcement, the storage modulus didn't change much as the strain increases. However, as the filler content increases, the modulus of the samples starts to drop with increasing oscillation strain, and for sample with 30 wt% of silica filler the effect is significant. This clearly demonstrates the existence of a filler-filler network in the filled elastomers. Different from the silica filled elastomers, oscillation sweep experiment on carbon black filled elastomers does not indicate an observable Payne effect until the carbon black content reaches 30 wt% (Figure 2.12, right). This suggests that the carbon

black is much easier to disperse into the polymer matrix and the filler-filler network between carbon black particles is weaker compared to that of fumed silica particles.

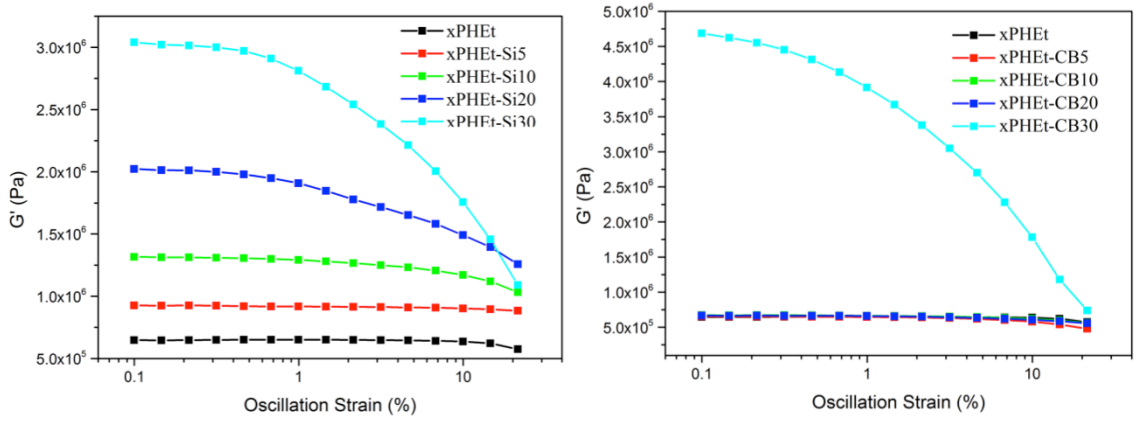


**Figure 2.12**

Oscillation sweep of xPHEt with fumed silica and carbon black filler.

## **2.2.6 Mechanical Properties**

### **2.2.6.1 Tensile Properties**

The tensile strengths for both fumed silica and carbon black filled elastomers are significantly higher than the unfilled elastomers. For example, the tensile strength of sample with 30 wt% of silica filler is about ten times higher than the sample with no filler at about 12 Mpa. Moreover, for samples with 30 wt% of filler, 2.5–5x increases in the moduli as compared to the unfilled samples we observed. However, at lower filler content, the moduli for both fumed silica and carbon black filled elastomers were only slightly higher than that of the parent elastomer. This suggests that under high filler content the formation of a percolating filler network contributes to the modulus of the elastomer. For fumed silica filled elastomers, their elongation at break values are about two times higher than the elastomer without filler, while for carbon black filled elastomers their elongation at break values are about the same as the sample without filler.

To further compare the mechanical properties of our materials with cured silicone elastomers, we prepared a baseline material from commercially available LSRs. These LSRs contain between 20~30 wt% of fumed silica; however, detailed information about the characteristics of this filler was not provided. As shown in Table 2.2, compared to the tensile properties of the crosslinked LSR, the synthesized polyethylene elastomers with both 30 wt% of fumed silica and carbon black filler have higher elastic modulus, and the sample with 30 wt% of silica filler has an even higher tensile strength. However, the LSR has a higher elongation at break value compared to the filled elastomers we synthesized.



**Table 2.2**Mechanical properties of filler reinforced prepolymers and LSR.<sup>a</sup>

Sample	Tensile <sup>b</sup>			Tear <sup>c</sup> N/mm	Hysteresis <sup>d</sup>	
	$\epsilon_b$ (%)	$\sigma_{TS}$ (Mpa)	E (Mpa)		Cycle 1 (%)	Cycle 2 (%)
xPHEt	94±4	1.3±0.1	2.6±0.2	0.68, 0.57	18.0, 17.5	12.1, 11.7
xPHEt-Si5	249±33	3.5±0.5	3.0±0.2	1.06, 1.01	15.2, 16.0	7.4, 7.4
xPHEt-Si10	252±21	3.6±0.4	2.6±0.1	1.20, 1.18	19.5, 13.4	8.5, 8.5
xPHEt-Si20	272±33	10.4±1.2	7.2±1.5	1.49, 1.63	41.5, 40.4	15.6, 15.6
xPHEt-Si30	168±26	12.2±1.4	16.5±1.6	1.82, 1.76	50.3, 46.3	23.2, 21.9
xPHEt-CB5	103±13	2.1±0.2	4.1±0.1	0.59, 0.67	6.9, 6.5	2.3, 3.2
xPHEt-CB10	113±14	2.6±0.2	4.3±0.3	0.87, 1.65	11.0, 10.5	3.9, 3.6
xPHEt-CB20	134±10	3.7±0.4	5.5±0.1	2.34, 1.85	23.8, 25.9	14.2, 12.8
xPHEt-CB30	92±12	5.1±0.7	10.0±0.3	2.32, 2.65	35.2, 35.0	20.9, 21.6
LSR <sup>e</sup>	455	9.5	3.0	--	26.6, 24.1	12.9, 12.0

<sup>a</sup> Mechanical properties measured on ASTM D1708 micro-tensile bars. <sup>b</sup> Measured at 69 mm/min, at least 4 tensile bars were tested for each sample. <sup>c</sup> Measured at 100 mm/min, 2 bars were tested for each sample ( 2'' x 0.5'' geometry samples with a 1'' cut). <sup>d</sup> Measured at 60 mm/min, strains no greater than 50% of the elongation at break, 2 bars were tested for each sample. <sup>e</sup> The crosslinked LSR was prepared by a two component LSRs. The two LSRs, Elastosil® LR 3003/60/A and 3003/60/B, were provided by Wacker Chemie AG.; component A is PDMS functionalized with vinyl pendent groups, while component B is functionalized with silane pendent groups. These two components

were mixed in a 1:1 wt% ratio and cured by press molding using similar conditions as those for the polyolefin elastomers.

### 2.2.6.2 Tear Strength

As shown in Table 2.2, the tear strength also undergoes significant increase upon the addition of the filler. The xPHET with no filler has a low tear strength value of 0.6 N/mm, while the tear strength value of sample with 30 wt% of carbon black is about 3 times higher on average. According to the literature, the tear strength of LSR with about 30 wt% of silica filler is around 15 N/mm, much higher than the filled polyethylene samples we obtained.<sup>75</sup> The tear strength of an elastomer is related to the fracture energy that is required to tear through a unit area of the elastomer. The fracture energy ( $G_c$ ) is correlated to the individual chain properties and the network density of the elastomer, and can be expressed as the following relationship:

$$G_c = KM^{0.5}$$

in which  $M$  is the molar mass between crosslinking sites<sup>84</sup> and  $K$  is a pre-factor that describes the chain properties of the elastomer that varies with chemical nature of the polymer.<sup>85,86</sup> Therefore the fact that LSR has a higher tear strength could be explained by: 1) the higher network density of LSR, which is controlled by the amount of silane groups along the PDMS side chain, and 2) the inherent strength of PDMS chain is also higher than the polyethylene chains, since the Si-O bond has higher bond strength (give numbers here) than that of the C-C bond.

### 2.2.6.3 Hysteresis

The hysteresis study summarized in Table 2.2 shows that both fumed silica and carbon black filled elastomers have higher energy loss with increasing filler content during the elongation cycles. For silica filled elastomers, the average energy loss during the two testing cycles are 48.8% and 22.5%, about 2 times higher than the sample with 5 wt% of silica filler, and similar behaviors are observed for the carbon black filled elastomers. The increasing energy loss with higher filler content during the hysteresis experiment is a typical stress softening behavior of filled elastomers. This behavior is called Mullins effect and is caused by the detachment and slippage of chain segments that reached their limit of extensibility on the filler surface.<sup>82</sup> The observed Mullins effect indicates that there are polymer-filler interactions in both fumed silica and carbon black filled elastomers.

### **2.2.7 Reinforcing Mechanism.**

To further understand the filler reinforcing mechanism, we studied the filler volume fraction of the samples. Table 2.3 shows the density and filler volume fraction of the crosslinked prepolymers, their modulus, and apparent molar mass between crosslinks. Since the densities of two fillers are quite close, for samples that have the same weight percent of the filler, their densities and filler volume fraction are also close. The room temperature storage modulus increases with the addition of the filler, and the corresponding apparent molar mass between crosslinks decreases. Since the molar mass between chemical crosslink sites remains the same (all the samples are from a same prepolymer), this suggests that the filler aggregates serve as crosslinking sites inside the polymer matrix that contribute to the modulus of the filled elastomers.

**Table 2.3**

Characterization of filler reinforced crosslinked prepolymers.

Sample	Density (g/cm <sup>3</sup> ) <sup>a</sup>	Volume Fraction (%) <sup>b</sup>	G' @ 25 °C (Mpa) <sup>c</sup>	M <sub>e</sub> (Kg/mol) <sup>d</sup>
xPHEt	0.87	0	0.43	5.0
xPHEt-Si5	0.91	2.1	0.74	3.0
xPHEt-Si10	0.93	4.2	0.94	2.5
xPHEt-Si20	1.01	9.1	3.6	0.70
xPHEt-Si30	1.04	14.2	5.8	0.44
xPHEt-CB5	0.88	2.1	0.70	3.1
xPHEt-CB10	0.90	4.3	0.50	4.4
xPHEt-CB20	0.98	9.3	0.70	3.5
xPHEt-CB30	1.03	14.7	4.0	0.64

<sup>a</sup> Determined by a isopropanol/ethylene glycol density gradient column at 25 °C.

<sup>b</sup> Calculated using density of silica filler (2.2 g/cm<sup>3</sup>) and carbon black filler (2.1 g/cm<sup>3</sup>).

<sup>c</sup> Determined by a dynamic frequency sweep test at 25 °C, 6.81 rad/s using an 8 mm parallel plate geometry. <sup>d</sup> Apparent average effective molar mass between crosslinks  $M_e = \rho RT/G$  at 25 °C.

Figure 2.13 compares the storage modulus of crosslinked prepolymers with fumed silica particles with that predicted by Smallwood-Guth-Einstein equation, which describes the hydrodynamic reinforcement of the filler.<sup>82</sup> At low filler volume fraction the experimental result is quite close to the predicted value, however, as the filler content goes higher, the experimental becomes much higher than the predicted value, suggesting that other than hydrodynamic reinforcement, both filler-filler interaction and polymer-filler interaction contributes to the enhancement of mechanical properties of filled elastomers, as discussed in the above sections.

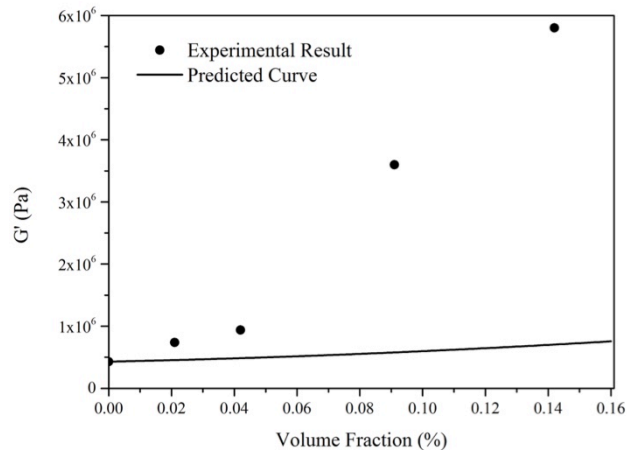


**Figure 2.13.**

Volume fraction-storage modulus relationship of xPHEt with silica filler. The predicted curve is plotted based on Smallwood-Guth-Einstein equation

$$G = G_0(1+2.5\phi+14.1\phi^2).$$

## **2.3 Conclusions**

In conclusion, saturated carboxy-telechelic polyethylene prepolymers were successfully synthesized and crosslinked with the addition of fumed silica and carbon black fillers. The mechanical properties of the filled elastomers are comparable with that of commercially available LSR in terms of their tensile strength and modulus, while the elongation at break and tear strength of LSR are still much higher than the filled polyolefin elastomer we obtained. The study on reinforcing mechanism under different strain scales suggests that the hydrodynamic effect, filler-filler interaction and polymer-filler interaction all contribute to the reinforcement of elastomers by filler addition.

## 2.4 Materials and Characterization

### 2.4.1 Materials

Cis-Cyclooctene (COE) (Fisher Scientific) was purified by distillation. Grubbs second generation (G2) catalyst, ethyl vinyl ether, and maleic acid were purchased from Sigma-Aldrich and used as received. Trimethylolpropane tri(2-methyl-1-aziridine propionate) (TAz, 95% purity) and Silica-supported platinum catalyst were obtained from PolyAziridine LLC and Dow Chemical Company respectively and used as received. 3-Ethyl-1-cyclooctene was synthesized according to the previous report.<sup>1</sup> Tetrahydrofuran and cyclohexane were purified with an M. Braun solvent purifications system and degassed with argon flow for 15min before used. Two types of fillers, Aerosil R-812 (hydrophobic fumed silica, surface area 260 m<sup>2</sup>/g, produced by Evonik) and V7H (low structure carbon black, surface area 112 m<sup>2</sup>/g, produced by Cabot) were used as received.

### 2.4.2 Characterization

<sup>1</sup>H and <sup>13</sup>C NMR spectra were recorded on a Bruker AV500 spectrometer at room temperature using CDCl<sub>3</sub> as solvent. Number-average molecular weight (M<sub>n</sub>) was determined by <sup>1</sup>H NMR end group analysis. Differential Scanning Calorimetry was performed on a TA Instruments Discovery DSC. Thermal gravimetric analysis was performed on a TA Instruments Q500 TGA. Density of filled elastomers was determined by a density gradient column (isopropanol/ethylene glycol) at room temperature (25 °C). Tensile, tear and hysteresis tests of filled elastomers were conducted on a Trapezium X



tensile tester (SHIMADZU) according to the ASTM D1708 standard. Dynamic Mechanical Temperature Analysis was performed by torsion test on a rectangular geometry (13mm x 50 mm x 1mm) using an ARES-G2 rheometer (TA Instruments). During the experiment temperature was increased from -90 to 200 °C at a rate of 5 °C/min. The frequency and strain were constant at 6.28 rad/s and 0.05%, respectively. Viscosity, dynamic frequency sweeps and oscillation sweeps were performed in an 8 mm parallel plate geometry using an ARES-G2 rheometer (TA Instruments). Scanning electron microscope was performed on HIACHI 4700 FE-SEM.

## 2.5 References

- (1) Hiemenz, P. C.; Lodge, T. *Polymer chemistry*; 2nd ed.; CRC Press: Boca Raton, 2007.
- (2) Bontems, S. L.; Stein, J.; Zumburum, M. A. *J Polym Sci Pol Chem* **1993**, *31*, 2697.
- (3) Delebecq, E.; Hermeline, N.; Flers, A.; Ganachaud, F. *Acs Appl Mater Inter* **2012**, *4*, 3353.
- (4) Delebecq, E.; Ganachaud, F. *Acs Appl Mater Inter* **2012**, *4*, 3340.
- (5) Martinez, H.; Hillmyer, M. A. *Macromolecules* **2014**, *47*, 479.
- (6) Winkler, B.; Rehab, A.; Ungerank, M.; Stelzer, F. *Macromol Chem Phys* **1997**, *198*, 1417.
- (7) Kobayashi, S.; Macosko, C. W.; Hillmyer, M. A. *Aust J Chem* **2010**, *63*, 1201.
- (8) Kobayashi, S.; Kim, H.; Macosko, C. W.; Hillmyer, M. A. *Polym Chem-Uk* **2013**, *4*, 1193.
- (9) Hillmyer, M. A.; Laredo, W. R.; Grubbs, R. H. *Macromolecules* **1995**, *28*, 6311.
- (10) Bielawski, C. W.; Grubbs, R. H. *Angew Chem Int Edit* **2000**, *39*, 2903.
- (11) Wypych, G. *Handbook of fillers*; 3rd ed.. ed.; Toronto : ChemTec Pub.: Toronto, 2010.
- (12) Yin, C. J.; Zhang, Q. Y.; Gong, D. L. *Polym Composite* **2014**, *35*, 1212.
- (13) Dorigato, A.; Pegoretti, A.; Fambri, L.; Slouf, M.; Kolarik, J. *J Appl Polym Sci* **2011**, *119*, 3393.
- (14) Vilgis, T. A. *Polymer* **2005**, *46*, 4223.

- (15) Stockelhuber, K. W.; Svistkov, A. S.; Pelevin, A. G.; Heinrich, G. *Macromolecules* **2011**, *44*, 4366.
- (16) Vilgis, T. A.; Heinrich, G.; Klüppel, M.; Knovel (Firm); Cambridge University Press, Cambridge, UK ; New York, 2009, p xii.
- (17) Raos, G.; Moreno, M.; Elli, S. *Macromolecules* **2006**, *39*, 6744.
- (18) Genesky, G. D.; Cohen, C. *Polymer* **2010**, *51*, 4152.
- (19) Gent, A. N.; Tobias, R. H. *J Polym Sci Pol Phys* **1982**, *20*, 2051.
- (20) Hamed, G. R. *Rubber Chem Technol* **1991**, *64*, 493.

## **Bibliography**

I grew up from Jin Zhou, Liao Ning Province, China. After high school I attended Zhejiang University and chose my major as polymer materials and engineering. My undergraduate research focused on the synthesis and modification of polyphosphazene under the supervision of Professor Xiao-jun Huang. I got my bachelor's degree in 2012 and after that I became a materials science graduate student in Department of Chemical Engineering at University of Minnesota and joined the research group of Professor Marc A. Hillmyer. My research focuses on the synthesis and application of polycyclooctene derivatives via ring-opening metathesis polymerization.